Proceeding of International Joint Conference on UNESA

Membrane Inovation for Proton Exchange Membrane Fuel Cells (PEMFCs) Based on Duck Feather Keratin Extract as Environmentally Friendly and Efficient Alternative Energy

Retno Asih*[1], Muhammad[1], Oktab Bahar Rahmadani[1], Melyana Putri Tiyarno[1], Diah Suci Lestari[1], and Indah Dwi Sasmitaningrum[1]
[1]* Institut Teknologi Sepuluh Nopember, Surabaya, Indonesia

Keywords:
Fuel Cell
Membrane
Duck Feather
Keratin

ABSTRACT

The interest in renewable and sustainable energy is increasing because it offers a clean and environmentally friendly approach. One system that produces renewable energy is a fuel cell, which produces electricity through electrochemical reactions. In fuel cells, the membrane has an important role in delivering the protons produced from the anode to the cathode. The membrane used can be replaced with an alternative membrane. Recent research into alternative 'green' membranes has become an exciting area of study. In this research, a proton-conducting keratin-based membrane was made from duck feather waste. Duck feather keratin extraction is carried out by dissolving the feathers in an alkaline solution and precipitating the supernatant obtained at the triple point. The phases contained in duck feathers and dry keratin that have been prepared, have been researched and are known to be related to the amide functional group which has an a-helical and β-sheet structure. Dry keratin exhibits agglomerated flat particles with a size of several microns. This indicates the potential of keratin derived from duck feathers for applications in fuel cell membranes.

INTRODUCTION

To support Indonesia's commitment to realize net zero emissions by 2060, efforts are needed to provide electrical energy that is environmentally friendly, renewable and efficient (Berghuis,2020). One of the technologies to produce green electricity in the future is fuel cell. Fuel cell is an electrochemical device that reacts hydrogen and oxygen with by-products of heat and water without any combustion process. Fuel cell technology is similar to batteries. The difference lies in the fuel cell system which is designed to have energy continuously (Safitri, 2016).

The type of fuel cell that is currently a global interest is PEMFCs (Proton Exchange Membrane Fuel cells) because it has a high current density, is easily distributed, and operates at low temperatures (Soon, 2023). In the PEMFCs system, the electrolyte used is a nafion-based membrane. However, the use of this membrane has several disadvantages, including not being environmentally friendly because it contains fluorine elements, and has high methanol diffusion from the anode so that it can reduce fuel cell efficiency (Safitri, 2016). Therefore, alternatives to nafion membranes are needed that are safer for the environment. One of them is keratin-based membrane material (Ma, 2016). Keratin contains cysteine which can be converted into sulfonic acid groups through post-oxidative treatment to obtain proton conductivity properties so as to produce membranes that can be applied to fuel cells (Ma, 2016).

Research related to keratin extraction from chicken feathers has been conducted by researchers from Nanyang Technological University (NTU) and produced Open Circuit

Voltage between 0.95 - 1 V with a maximum power of 25 mW which is able to turn on LED lights (Ma, 2016). However, until now, there has been no research on the utilization of keratin from duck feathers as a fuel cell membrane material. Duck feathers have keratin content equivalent to chicken feathers (~97%) and contain preening oil that can improve the hydrophilic or hydrophobic properties of the membrane (Dewi, 2021) The potential of duck feathers as an environmentally friendly fuel cell membrane material is enormous. In addition, the high interest of Indonesian people in raising and consuming processed duck produces significant duck feather waste. Based on BPS data, the duck population in Indonesia reached 58,243,335 heads in 2020 with the percentage of feathers in each cutting as much as 6% of the live weight (Sharma, 2018). The addition of duck feather keratin-based membranes to Fuel Cells is expected to produce alternative energy that is environmentally friendly and efficient. In this Program Kreativitas Mahasiswa – Riset Eksakta (PKM-RE), research is aimed at knowing the potential of duck feather keratin extract as a fuel cell membrane material in an effort to produce environmentally friendly and efficient alternative energy. The addition of duck feather keratin-based membranes to Fuel Cells is expected to produce optimal conductivity as in the use of synthetic membranes. In addition, several tests were carried out to determine the structure and performance of the membrane formed, namely X-Ray Diffraction (XRD), Scanning Electron Microscophy-Energy Dispersion X-Ray (SEM-EDX), Fourier Transform Infrared (FTIR), and Electrochemical Impedance Spectroscopy (EIS).

RESEARCH METHOD
The duck feathers used in this research came from a local market in Surabaya, Indonesia. The duck feathers were first washed to remove dirt and then dried in the sun. The calamus and rachis were manually separated to obtain the soft part of the feather known as the vane (Njoku, et al., 2019). The collected feathers are then minced to obtain fine feather fiber. A schematic of the process in preparing duck feathers before keratin extraction is shown in Figure 1(a).
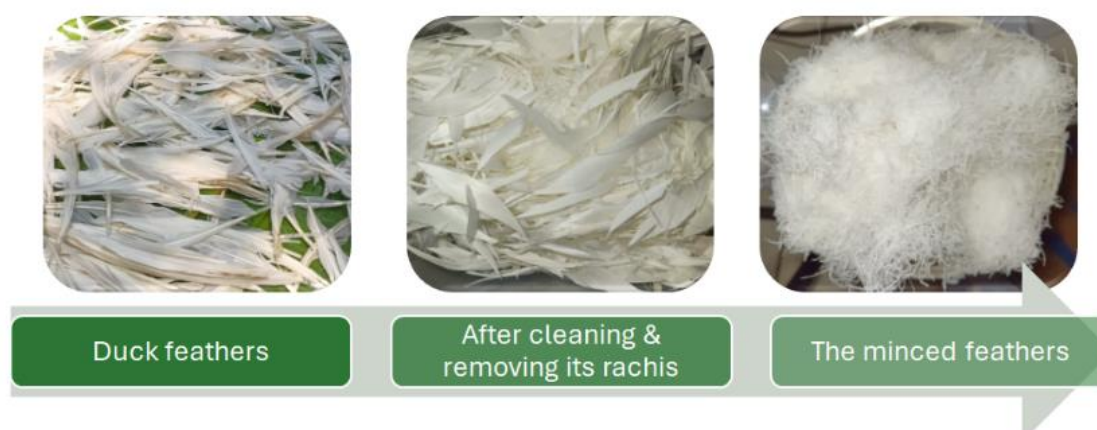

Figure 1. Process scheme (a) dries the duck feathers in the sun (b) separates the feather from its calamus and rachis, and (c) minces the duck feathers.

Keratin Extraction from Duck Feathers

The working steps in utilising duck feather keratin extraction, namely 14.4 g of duck feather waste was collected and soaked in water for fifteen minutes, to minimise dirt. Then washed with soap water and dried. The dried duck feathers were blended, then stored in a closed container and tested for FTIR, SEM-EDX, and XRD. A total of 14.4 grams of fine duck feathers were added to a solvent (8M urea, 10% l-cysteine by weight of duck feathers, 50%NaOH) with a pH of 13, and heated using a hot plate at 75°C with a stirrer speed of 550 rpm for twelve hours. Then the solvent was filtered and centrifuged at 10000 rpm for twenty minutes. The supernatant was added with hydrochloric acid and sodium sulphate until it reached pH 4, and formed a precipitate. The precipitate formed was filtered and washed with distilled water for three repetitions. The fresh keratin solids obtained were collected and weighed. Afterwards, FTIR, XRD, and SEM-EDX tests were carried out on the powder solids.

Duck Feather Membrane Fabrication

In making the membrane, fresh keratin was added to solvent (0.1M sodium carbonate and sodium bicarbonate) with the ratio of keratin and solvent (15:85)%. The mixture was then added SDS with variations of 40% and 60% of the weight of dried keratin. Subsequently, the mixture stood for 24 hours at room temperature. The mixture was heated by microwave at 90°C for one hour, after which glycerol was added as much as 10% of the weight of dried keratin and the mixture was heated again at 60°C. The membrane was incubated in solution (10% ethanol, 10% acetic acid) and 10% glycerol from the solution before further use.

Characterisation

Membrane characterisation was carried out by XRD testing to observe the phases formed, FTIR to analyse chemical bonds and functional groups, DSC/TGA to determine heat characteristics, and SEM/EDX to observe the morphology and elemental content of the membrane. In addition, EIS test was conducted to determine the conductivity of the sample. The voltage effectiveness test begins by connecting the fuel cell electrode equipped with a duck feather keratin membrane to an electric cable. Afterwards, the cable was connected to a digital multimeter to measure the amount of voltage. The multimeter used, the UX-389 type, has AC and DC current measurements with resistance of 200 ohms to 200 kilo ohms. Furthermore, data processing is carried out using the formula for current strength, voltage, and electrical power so that the data generated after processing can show the effectiveness of the fuel cell.

RESULTS AND DISCUSSION

Development of learning media (overlay visualization)

The structure and thermal stability of duck feathers were examined prior to keratin extraction. Previous studies have indicated that duck feathers contain fibrous keratin, abundant in the barbs, calamus, and rachis, making them a suitable source for the production of high-value keratin-based products (Tesfaye, 2018). The structure of duck

feathers was first examined before extracting keratin and applying it as a precursor for preparing fuel cell membranes. Figure 2(a) displays the FTIR spectrum of duck feathers, showing the presence of amide-A, amide-I, amide-II, and amide-III functional groups at wavenumbers 3264.4, 1620.9, 1532.8, and 1235.0 cm-1, respectively. Additional peaks were also observed, associated with symmetric CH3 stretching at 2959.5 cm-1, CH2 scissoring at 1448.4 cm-1, and C-S stretching at 595.2 cm-1. This spectrum is consistent with those previously reported for French mullard duck feathers (Tesfaye, 2018) and chicken feathers (Dewi, 2021 and Alvarez, 2023) The observed peaks and their assignments are listed in Table 1.
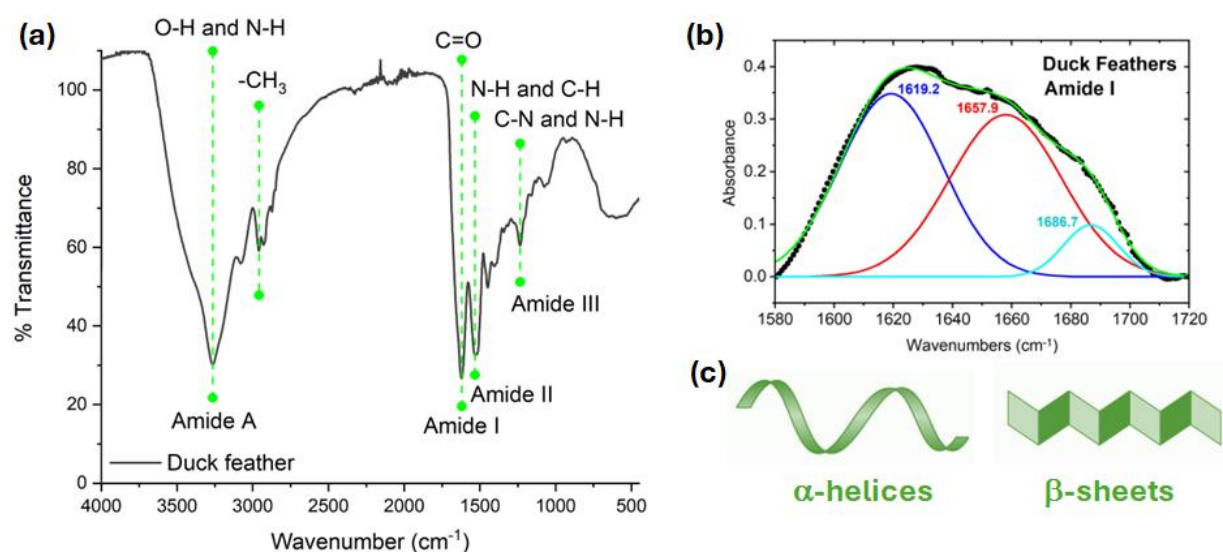

Figure 2. (a) FTIR spectrum of duck feathers. (b) Deconvolution of the spectrum within Amide I region. (c) Illustrations of α-helices and β-sheets.

Table 1. Summary of the observed FTIR peaks and their assignments, consistent with the previous reports in (Dewi, 2021), (Tesfaye, 2018), (Alvarez, 2023)

Wave Number (cm^{-1})	Assignment
3264.44	O-H and N-H stretching (Amide A)
2959.50	Symmetrical CH$_3$ stretching
1620.97	C=O stretching (Amide I), containing of a-helices (46.9 %), β-sheets (45.9 %), and turns (7.2 %)
1532.87	N-H bending and C-H stretching (Amide II)
1448.43	CH$_2$ scissoring
1235.04	C-N stretching and N-H in plane bending (Amide III)
595.20	C-S stretching

The Amide-I peak of duck feathers was deconvoluted to further examine the secondary structure of the protein. As shown in Figure 2(b), the deconvolution resulted in three peaks at 1619.2, 1657.9, and 1686.7 cm-1, corresponding to α-helices, β-sheets, and turns, respectively. An illustration of the α-helices and β-sheets structures is displayed in Figure

2(c). The relative percentage (%fraction) of each structure was estimated from the area of each peak. It was found that the %fraction as shown in Table 2.

Table 2. Summary of the FTIR deconvolution spectrum in Amide I region

Wave Number (cm^{-1})	Assignment	%Fraction
1619.2	β -sheet + random coil	46.9
1657.9	α -helix	45.9
1686.7	Turns	7.2

Figure 3(a) is the XRD pattern of duck feathers shows a broad peak from ~9° to ~20°. The first part is related to α-helices, and the latter has an asymmetric shape resulting from overlapping peaks between α-helices at 17.8° and β-sheets at 19.5°. The XRD pattern of duck feathers closely resembles the XRD pattern of chicken feathers (Ma, et al., 2016), confirming the presence of the protein secondary structure from the FTIR analysis. Additionally, the broad peak feature indicates a low degree of crystallinity in duck feathers. The crystalline index (Cr×I) is determined by the ratio of the crystalline peak area to the total area. The estimated Cr×I is approximately 0.47, meaning that ~47% of duck feathers consist of crystalline α-helices and β-sheets, and the remaining ~53% is amorphous phase. The Cr×I of duck feathers is comparable to that observed in chicken feathers (Dewi, 2021).
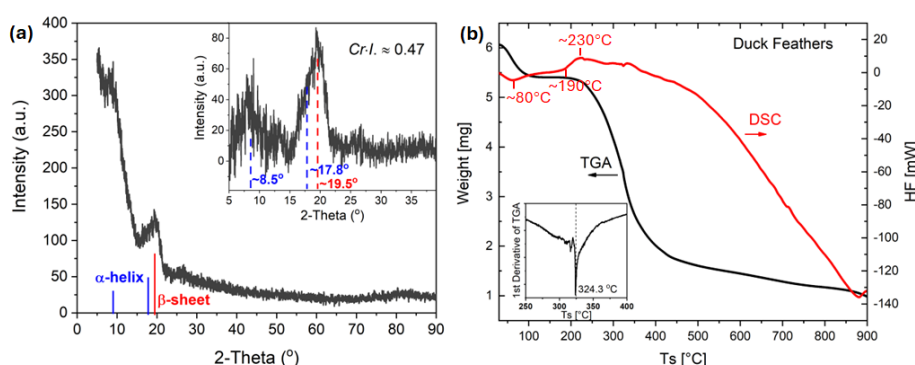

Figure 3. (a) XRD pattern of duck feathers. Inset is a close view of the baseline-subtracted pattern within 5°-39°. (b) DSC/TGA curves of duck feathers under N2 atmospheric gas.

The thermal stability of duck feathers was examined using DSC/TGA curves, as presented in **Figure 3(b)**. A broad, low-intensity endothermic peak is visible on the DSC graph. A broad dip below 100 °C indicates the amount of water bound within the keratin structure of duck feathers, and another dip is observed at ~200 °C, implying the melting of the crystalline keratin structure. A small exothermic peak at ~230 °C is associated with the irregular decomposition of α-helices. These results are consistent with those reported for chicken feathers (Tesfaye, et al., 2018). TGA analysis confirms two weight loss steps, the first being ~11% at temperatures below 100 °C, and the second being a substantial weight loss (~63%) at 200-400 °C, similar to what occurs in chicken feathers.

Structural Analysis of Dried Keratin

Figure 4(a) is the XRD pattern of dried keratin shows peaks from ~9° to ~20°. The α-helices are present at peaks around ~9° and ~17.3°, while the β-sheets are present at a peak around ~19.4°. Peaks marked with (*) indicate sulfur, hypothesized to be derived from the Na_2SO_4 precursor. The peaks observed in dried keratin are narrower compared to those in duck feathers, indicating that dried keratin has higher crystallinity than duck feathers. In Figure 4(b), the FTIR spectrum of dried keratin shows the presence of amide A, amide I, amide II, and amide III groups, similar to those in duck feathers, with the addition of CH_2, C-O, C-S, and C-S-C groups. Figures 5(a) and 5(b) show magnified images of dried keratin. Figure 5(c) represents the data in Figure 5(d), which shows that carbon (C) is the most abundant element in the keratin structure, with a weight percentage of 49.5% and an atomic percentage of 65.96%. The presence of sulfur (S) in the EDX data is hypothesized to originate from the Na_2SO_4 precursor.
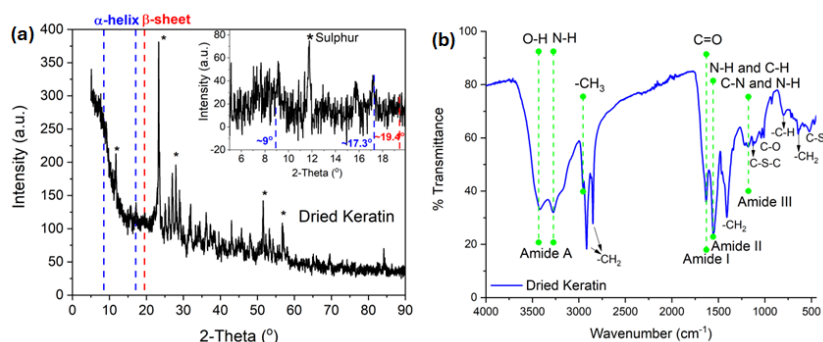

Figure 4. (a) XRD pattern and (b) FTIR spectrum of dried keratin extracted from duck feathers. Inset in (a) is the enlarged view of the XRD pattern within 5°-20°.
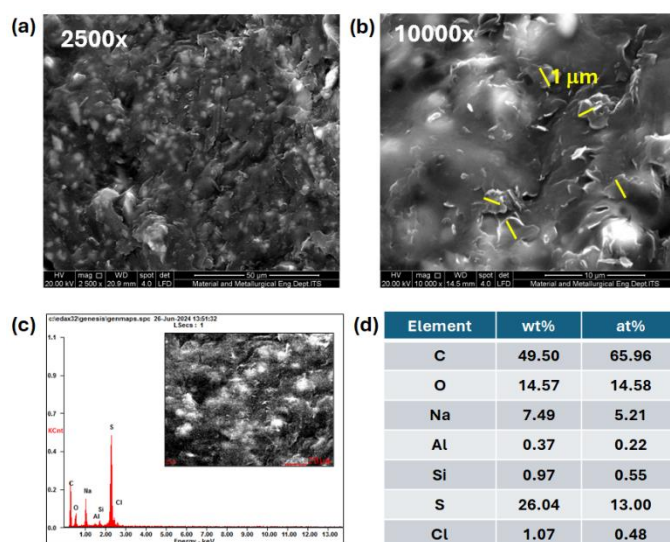

Element	wt%	at%
C	49.50	65.96
O	14.57	14.58
Na	7.49	5.21
Al	0.37	0.22
Si	0.97	0.55
S	26.04	13.00
Cl	1.07	0.48

Figure 5. SEM micrographs of dried keratin with the magnifications of (a) 2500× and (b) 10000×. (a) EDX graph of the observed SEM micrograph (inset) and (d) its elemental component.

Electrical Properties

Measurements using a multimeter on both processed and unprocessed duck feather samples showed that neither sample's resistance, current, nor voltage could be measured. This indicates that both processed and unprocessed duck feathers are insulative and do not conduct electrical current. The impedance data for duck feathers and dried keratin form semicircular graphs. The radius of the semicircle is related to the resistivity of the sample. A smaller radius indicates higher conductivity of the sample. Dried keratin has higher conductivity than duck feathers. This is because conductivity is closely related to the density of the sample. Dried keratin is in the form of agglomerated granules, whereas duck feathers are in the form of fibers, which are not as dense as dried keratin. The real impedance (Z') of the membrane is higher compared to that of dried keratin. This indicates that the membrane offers more resistance to the flow of alternating current than dried keratin. The electrical conductivity of the membrane is lower than that of dried keratin. This suggests that the membrane is less efficient at conducting electricity compared to dried keratin, likely due to its material properties and structure. There is a need to assess and possibly improve the fabrication process of the membrane. The current method may be leading to suboptimal electrical properties, affecting its performance. Membranes containing 60% SDS (sodium dodecyl sulfate) exhibited random impedance data, which is not displayed. This randomness is hypothesized to result from the membrane becoming highly insulative, indicating that a high concentration of SDS may adversely affect the membrane's conductivity.
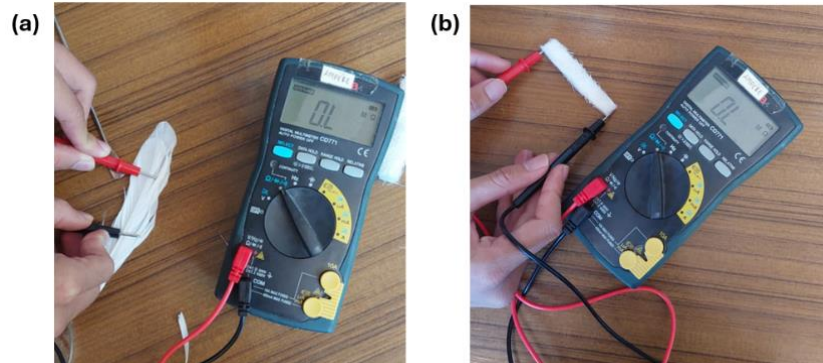

Figure 6. Resistance of duck feathers (a) before compression and (b) after compression.
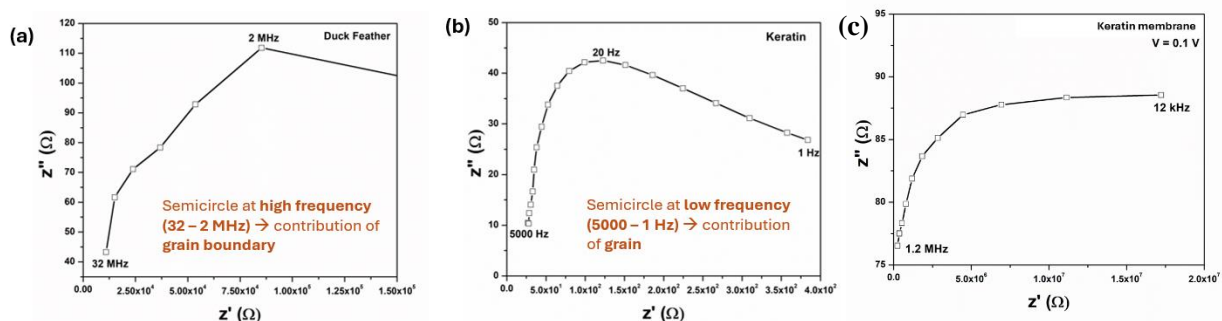

Figure 7. Impedance of (a) duck feathers (b) dried keratin and (c) keratin membrane with 40% SDS variant.

CONCLUSION

Duck feathers, whether treated or untreated, are inherently insulative. However, when processed into a keratin extract solution, the solution exhibits better conductivity compared to untreated duck feathers. Extraction of dry keratin from duck feathers produces keratin that is more conductive than unextracted duck feathers. The resulting membranes have lower electrical conductivity compared to dry keratin.

REFERENCES

Alvarez, S., Raydan, N. D. V., Svahn, I., Gontier, E., Rischka, K., Charrier, B., & Robles, E. (2023). Assessment and characterization of duck feathers as potential source of biopolymers from an upcycling perspective. Sustainability, 15(19), 14201.

Berghuis, N. T., Zulfikar, M. A., & Wahyuningrum, D. (2020). Sintesis membran komposit berbahan dasar kitosan dengan metoda sol-gel sebagai membran fuel cell pada suhu tinggi. al Kimiya: Jurnal Ilmu Kimia dan Terapan, 7(1), 35–46.

Dewi, A. T. (2021). Sistem pakar diagnosa penyakit pada bebek menggunakan metode. Tesis, 1.

Kementerian Perekonomian. (2023). Miliki perhatian serius pada energi baru terbarukan, pemerintah berkomitmen menjaga ketersediaan energi nasional berkelanjutan. Retrieved from https://www.ekon.go.id/publikasi/detail/5250/miliki-perhatian-serius-pada-energi-baru-terbarukan-pemerintah-berkomitmen-menjaga-ketersediaan-energi-nasional-berkelanjutan.

Ma, B., Qiao, X., Hou, X., & Yang, Y. (2016). Pure keratin membrane and fibers from chicken feather. International Journal of Biological Macromolecules, 89, 614–621.

Safitri, I. A., Rudiyanto, B., Nursalim, A., & Hariono, B. (2016). Uji kinerja smart grid fuel cell tipe proton exchange membrane (PEM) dengan penambahan hidrogen. Jurnal Ilmiah Inovasi, 1(1), 11–16.

Sharma, S., Gupta, A., Kumar, A., Kee, C. G., Kamyab, H., & Saufi, S. M. (2018). An efficient conversion of waste feather keratin into ecofriendly bioplastic film. Clean Technologies and Environmental Policy, 20(10), 2158–2162.

Soon, W. L., Peydayesh, M., Wild, T. D., Donat, F., Saran, R., Müller, C. R., Gubler, L., Mezzenga, R., & Miserez, A. (2023). Renewable energy from livestock waste valorization: Amyloid-based feather keratin fuel cells. Energy, Environmental, and Catalysis Applications, 4(1), 309–313.

Tesfaye, T., Sithole, B., Ramjugernath, D., & Mokhothu, T. (2018). Valorisation of chicken feathers: Characterisation of thermal, mechanical and electrical properties. Sustainable Chemistry and Pharmacy, 9, 27–34.

Rigid Body Motion: The End Effector of 4-DoF Robot Motion Analysed by Denavit Hartenberg Method

L P B Yasmini[1*], I N W Artha[1], I G A Gunadi[1]

[1,*] Universitas Pendidikan Ganesha, Singaraja, Indonesia

ABSTRACT

Keywords:
Rigid body
Denavit Hartenberg
Robot Motion
Transformation matrix

Rigid body motion is consist of two kinds motion which are rotational and translational motion, as an example is a robot kinematic motion. Robot forward kinematics refers to its final position (end effector), which combines rotational and translational motion along its trajectory. This research is a theoretical physics study that aims to analyze the end effector of a robot arm with four degrees of freedom (4-DoF) using the Denavit Hartenberg (DH) method and visualize the motion by using Simulink (DH-parameters) in MATLAB. This research was carried out through manual analysis and visualization of the equations obtained. This research provides the transformation matrix g_st (θ) as a forward kinematics equation and visualize the motion by MATLAB.

INTRODUCTION

One type of robot widely used on an industrial scale is the robotic manipulator (Faiq, et al., 2022; Suddin, et al., 2017) The development of robot manipulators is expected to make work easier and more efficient. In general, a robot manipulator is composed of an arm (link), a joint, and a hand (as an end-effector) in the form of a hand with a finger (gripper) and degrees of freedom (DoF) as a combination of movements from each joint. (joints). Many studies have been carried out related to the development of robotic manipulator systems (Faiq, et al., 2022; Suddin, et al., 2017; Ge, 2022; Gallardo-Alvarado, et al., 2018; Purwanto, et al., 2020; Salman and Roman, 2022; Kucuk and Bingul, 2006; Serrezuela, et al., 2017)

Research conducted by Utomo and Munadi (2013) stated that the motion of robot manipulators is carried out by analyzing robot kinematics. Research from Ge (2022) analyzes robot kinematics using screw theory, Newton Raphson's method, and DH parameters in MATLAB, showing that this method has high accuracy and is more practical for analyzing forward kinematics on a robot arm (manipulator) with 7 degrees of freedom. The results of a study by Andika and Salamah (2018) state that the analysis of forward and reverse kinematics on a robotic arm (manipulator) with 3 degrees of freedom can be completed using the DH-parameters. This research was obtained using MATLAB and RoboAnalyzer software, which shows that the DH-parameters can formulate forward kinematics and reverse kinematics on a robot arm (manipulator) with 3 degrees of freedom and produce the same matrix from manual calculations or via MATLAB and RoboAnalyzer software.

Generally, robot motion can be analyzed based on the concept of motion in Physics, i.e., the concept of motion of a rigid body. The system's motion is said to be a rigid body motion if the distance between points on each body does not change during the motion. This concept is becoming the basic concept to analyze the motion of robotic manipulators

(Murray, et al., 1994; Yasmini and Gunadi, 2012). This research analyses the basic concepts of kinematics in robot arm movement using DH-parameters and visualizes by using MATLAB.

RESEARCH METHOD
This research is a theoretical physics study carried out through a literature review of previously developed procedures, analyses manually to obtain an equation. Next, to compare the results and visualize the equation, thus providing an overview of the form of the equation that has been studied. The research method used is a literature study and manual analysis, which are then visualized using MATLAB.

RESULTS AND DISCUSSION
Robot Manipulator 4-DoF and Denavit Hartenberg Related Parameters
In this study, the author analyses the basic concepts of robot kinematics in moving a robot arm (manipulator) with 4-DoF using the DH parameters represented in Figure 1.
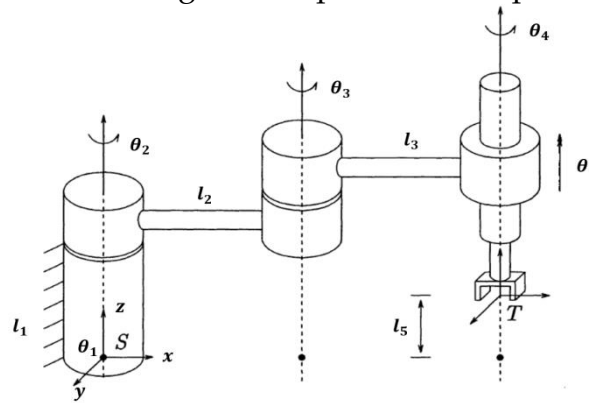

Figure 1. Robot manipulator with 4-DoF [10]

The representation of a robot manipulator with 4-DoF in Figure 1 shows that the system configuration consists of a pair (p_{st}, R_{st}) where p_{st} shows the movement journey until the end effector point of the robot is found or can be called a position vector in the T frame which originates from the frame S. So that the motion of a rigid body can be represented using a rigid body transformation to describe the instantaneous position and orientation of the body's coordinate frame relative to the fixed frame. A rotation matrix that represents the movement configuration of point S towards point T is represented by $g_{st} \in SO(3)$, so the mapping g_{st} can be expressed as follows.

$$g_{st}(\theta) = g_{l_0 l_1}(\theta_1) g_{l_1 l_2}(\theta_2) \cdots g_{l_{n-1}, l_n}(\theta_n) g_{l_n t}, = \begin{bmatrix} R(\theta) & p(\theta) \\ 0 & 1 \end{bmatrix} \qquad (1)$$

Equation (1) shows the relationship between the geometric concept of spatial joints in robots and the general coordinate concept used to determine the position of an object. The goal of kinematics is to define the relative position of a frame with its original coordinates. Based on this, Figure 2 represents the coordinate configuration of each frame on a robot manipulator with 4-DoF as follows,
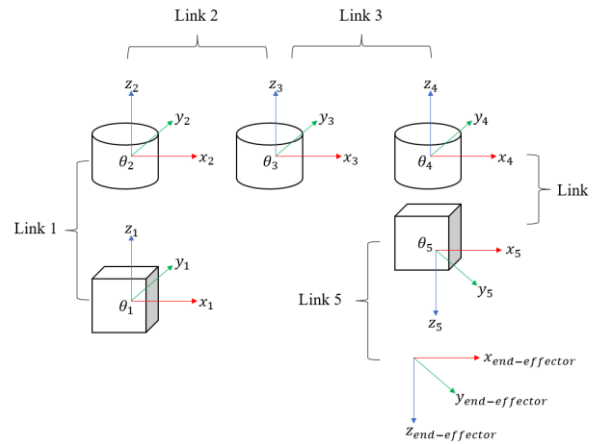
Figure 2. Configure the coordinates of each frame on the robot manipulator with 4-DoF

Figure 2 shows the angular position and direction of each joint and link movement, which can be determined using the concept of a rigid body. The motion of a rigid body consists of rotational motion about a straight line followed by translational motion on that straight line using exponential coordinates. Figure 2 also provides a representation of the primary frame (S or θ_1) and final frame or end effector (T) with the corresponding rotation coordinates at each joint of the robot, thus providing a complete parameterization of the kinematics of the robot.

An alternative parameterization, a standard commonly used in robotics, is the Denavit Hartenberg parameters [10]. The Denavit Hartenberg parameters in each homogeneous transformation g_{l_{i-1},l_i} according to equation (1), is represented by the product of four basic transformations, which can be seen in the following equations,

$$g_{l_{i-1},l_i} = Rot_{z,\theta_i} Trans_{z,d_i} Trans_{x,a_i} Rot_{x,\alpha_i} \tag{2}$$

$$g_{l_{i-1},l_i} = \begin{bmatrix} \cos\theta_i & -\sin\theta_i & 0 & 0 \\ \sin\theta_i & \cos\theta_i & 0 & 0 \\ 0 & 0 & 1 & 0 \\ 0 & 0 & 0 & 1 \end{bmatrix} \begin{bmatrix} 1 & 0 & 0 & 0 \\ 0 & 1 & 0 & 0 \\ 0 & 0 & 1 & d_i \\ 0 & 0 & 0 & 1 \end{bmatrix} \begin{bmatrix} 1 & 0 & 0 & a_i \\ 0 & 1 & 0 & 0 \\ 0 & 0 & 1 & 0 \\ 0 & 0 & 0 & 1 \end{bmatrix} \begin{bmatrix} 1 & 0 & 0 & 0 \\ 0 & \cos\alpha_i & -\sin\alpha_i & 0 \\ 0 & -\sin\alpha_i & \cos\alpha_i & 0 \\ 0 & 0 & 0 & 1 \end{bmatrix} \tag{3}$$

$$g_{l_{i-1},l_i} = \begin{bmatrix} \cos\theta_i & -\sin\theta_i\cos\alpha_i & \sin\theta_i\sin\alpha_i & a_i\cos\theta_i \\ \sin\theta_i & \cos\theta_i\cos\alpha_i & -\cos\theta_i\sin\alpha_i & a_i\sin\theta_i \\ 0 & \sin\alpha_i & \cos\alpha_i & d_i \\ 0 & 0 & 0 & 1 \end{bmatrix} \tag{4}$$

Based on equation (4), it is known that there are four parameters in Denavit Hartenberg, namely θ, α, d, and a are parameters from *the link i* and *joint* to i, which have been represented in Figure 2 regarding the coordinate configuration of each frame on the robot manipulator with 4-DoF. After determining the coordinates of each frame, determine the DH-parameters for the robot, shown in Table 1.

Proceeding of International Joint Conference on UNESA
Homepage : https://proceeding.unesa.ac.id/index.php/pijcu
e-ISSN : 3032-3762

PIJCU, Vol. 2, No. 2, June 2025
Page 1-8
© 2025 PIJCU:
Proceeding of International Joint Conference on UNESA

Table 1. DH-parameters for robot manipulator with 4-DoF motion

Link	θ	d	a	α	Information
1	0	l_1	0	0	Base
2	θ_2	0	l_2	0	Arm
3	θ_3	0	l_3	0	Arm
4	θ_4	0	0	180°	Arm
5	0	l_5	0	0	end-effector

3.2 Kinematic Analysis

The forward kinematics equation of motion of the robot arm under study can be formulated with the values given based on Table 1 regarding the DH-parameters of the coordinate configuration of each frame on the robot manipulator with 4-DoF. So, the homogeneous matrix transformation for each arm can be determined using equation (4) as follows. Matrix transformation for link 1 ($g_{l_{1,l_2}}$).

$$g_{l_{1,l_2}} = \begin{bmatrix} 1 & 0 & 0 & 0 \\ 0 & 1 & 0 & 0 \\ 0 & 0 & 1 & l_1 \\ 0 & 0 & 0 & 1 \end{bmatrix} \tag{5}$$

Matrix transformation for link 2 ($g_{l_{2,l_3}}$).

$$g_{l_{2,l_3}} = \begin{bmatrix} \cos\theta_2 & -\sin\theta_2 & 0 & l_2\cos\theta_2 \\ \sin\theta_2 & \cos\theta_2 & 0 & l_2\sin\theta_2 \\ 0 & 0 & 1 & 0 \\ 0 & 0 & 0 & 1 \end{bmatrix} \tag{6}$$

Matrix transformation for link 3 ($g_{l_{3,l_4}}$).

$$g_{l_{3,l_4}} = \begin{bmatrix} \cos\theta_3 & -\sin\theta_3 & 0 & l_3\cos\theta_3 \\ \sin\theta_3 & \cos\theta_3 & 0 & l_3\sin\theta_3 \\ 0 & 0 & 1 & 0 \\ 0 & 0 & 0 & 1 \end{bmatrix} \tag{7}$$

Matrix transformation for link 4 ($g_{l_{4,l_5}}$).

$$g_{l_{4,l_5}} = \begin{bmatrix} \cos\theta_4 & \sin\theta_4 & 0 & 0 \\ \sin\theta_4 & -\cos\theta_4 & 0 & 0 \\ 0 & 0 & -1 & 0 \\ 0 & 0 & 0 & 1 \end{bmatrix} \tag{8}$$

Matrix transformation for link 5 ($g_{l_{5,l_1}}$).

Proceeding of International Joint Conference on UNESA
Homepage : https://proceeding.unesa.ac.id/index.php/pijcu
e-ISSN : 3032-3762

PIJCU, Vol. 2, No. 2, June 2025
Page 1-8
© 2025 PIJCU:
Proceeding of International Joint Conference on UNESA

$$g_{l_{5},l_{1}} = \begin{bmatrix} 1 & 0 & 0 & 0 \\ 0 & 1 & 0 & 0 \\ 0 & 0 & 1 & l_5 \\ 0 & 0 & 0 & 1 \end{bmatrix} \tag{9}$$

The robot's forward kinematics can be described by referring to the position of the end effector, which is the result of rotational and translational movements along $p(\theta)$ or $p(x)$, $p(y)$ and $p(z)$ (position vectors in the transformation matrix) according to equation (1). So, the homogeneous transformation matrix produced for joint movement from the base to the end effector can be written as follows,

$$g_{st}(\theta) = g_{l_1 l_2}(\theta_2) g_{l_2 l_3}(\theta_3) g_{l_3 l_4}(\theta_4) g_{l_4 l_5}(\theta_5) g_{l_5 l_1}(\theta_1)$$

$$g_{st}(\theta) = \begin{bmatrix} \cos(\theta_2 + \theta_3 + \theta_4) & \sin(\theta_2 + \theta_3 + \theta_4) & 0 & l_3 \cos(\theta_2 + \theta_3) + l_2 \cos\theta_2 \\ \sin(\theta_2 + \theta_3 + \theta_4) & -\cos(\theta_2 + \theta_3 + \theta_4) & 0 & l_3 \sin(\theta_2 + \theta_3) + l_2 \sin\theta_2 \\ 0 & 0 & -1 & -l_5 + l_1 \\ 0 & 0 & 0 & 1 \end{bmatrix} \tag{10}$$

The result of the transformation matrix $g_{st}(\theta)$ as equation (10) is a forward kinematics equation obtained using DH-parameters representing the kinematics of the rigid body, which is studied about the position and orientation of the frame attached to each link of the robot and then building a homogeneous transformation between the frames of the robot manipulator 4-DoF.

3.3 Visualization by MATAB

For visualizing the forward kinematics of the robot manipulator by MATLAB, the author entered Table 1 regarding the DH-parameters for the movement of the robot into the Robotic Toolbox by Peter Corke on MATLAB. As in equation (10), the rotation matrix with the associated angles used is a sum. Whereas the translation matrix is related to the arm's length and the rotation angles of the robot arm movement.

Based on that, it is necessary to create an initial position of the robot before it transforms. The initial state, chosen that l_1, l_2, l_3, and l_5 at 10 cm while θ_2, θ_3, and θ_4 at 0°. Then a state is obtained by determining the value of the DH-parameter in the transformation or a combination of movements of the robot (as in Figure 1 and Figure 2) to set the initial state as follows.

Table 2. DH-parameters describing the robot's initial position.

Link	θ	d	a	α	Information
1	0°	10 cm	0	0	Base
2	0°	0	10 cm	0	Arm
3	0°	0	10 cm	0	Arm
4	0°	0	0	180°	Arm
5	0°	10 cm	0	0	end-effector

Based on Table 2, regarding the DH-parameters for the transformation of the robot being studied, the homogeneous matrix transformation for each link or arm can be described using (10),

Proceeding of International Joint Conference on UNESA
Homepage : https://proceeding.unesa.ac.id/index.php/pijcu
e-ISSN : 3032-3762

PIJCU, Vol. 2, No. 2, June 2025
Page 1-8
© 2025 PIJCU:
Proceeding of International Joint Conference on UNESA

$$g_{st}(\theta) = \begin{bmatrix} \cos(\theta_2 + \theta_3 + \theta_4) & \sin(\theta_2 + \theta_3 + \theta_4) & 0 & l_3\cos(\theta_2 + \theta_3) + l_2\cos\theta_2 \\ \sin(\theta_2 + \theta_3 + \theta_4) & -\cos(\theta_2 + \theta_3 + \theta_4) & 0 & l_3\sin(\theta_2 + \theta_3) + l_2\sin\theta_2 \\ 0 & 0 & -1 & -l_5 + l_1 \\ 0 & 0 & 0 & 1 \end{bmatrix}$$

$$g_{st}(\theta) = \begin{bmatrix} cos(0° + 0° + 0°) & sin(0° + 0° + 0°) & 0 & 10\,cos(0° + 0°) + 10\,cos\,0° \\ sin(0° + 0° + 0°) & -cos(0° + 0° + 0°) & 0 & 10\,sin(0° + 0°) + 10\,sin\,0° \\ 0 & 0 & -1 & -10 + 10 \\ 0 & 0 & 0 & 1 \end{bmatrix}$$

$$g_{st}(\theta) = \begin{bmatrix} \cos(0°) & \sin(0°) & 0 & 10\cos(0°) + 10\cos 0° \\ \sin(0°) & -\cos(0°) & 0 & 10\sin(0°) + 10\sin 0° \\ 0 & 0 & -1 & 0 \\ 0 & 0 & 0 & 1 \end{bmatrix}$$

$$g_{st}(\theta) = \begin{bmatrix} 1 & 0 & 0 & 10 + 10 \\ 0 & -1 & 0 & 0 - 0 \\ 0 & 0 & -1 & 0 \\ 0 & 0 & 0 & 1 \end{bmatrix}$$

$$g_{st}(\theta) = \begin{bmatrix} 1 & 0 & 0 & 20 \\ 0 & -1 & 0 & 0 \\ 0 & 0 & -1 & 0 \\ 0 & 0 & 0 & 1 \end{bmatrix}$$

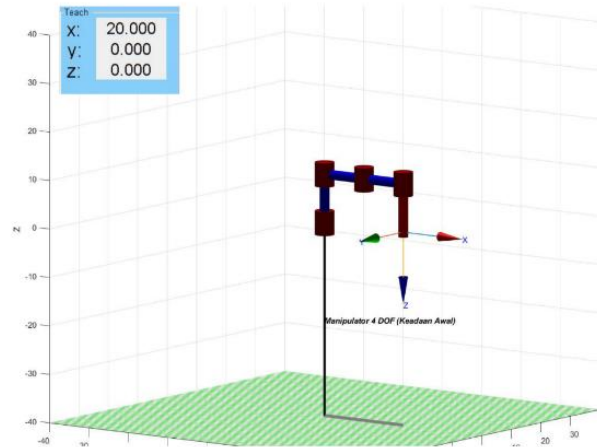Visualization of the initial position of the robot as shown in Figure 3.

Figure 3. Visualization of the robot's initial position

Figure 3 represents the results of the $g_{st}(\theta)$ transformation equation, that formed from the robot's initial position, that analyzed and visualized by MATLAB. Moreover, we can see that the x, y, and z-axes represent the output result as the end effector position of the robot, form the box we know that [20 0 0], respectively. So, this can be used as a comparison or validation of the correctness of the manual analyses that we have carried out.
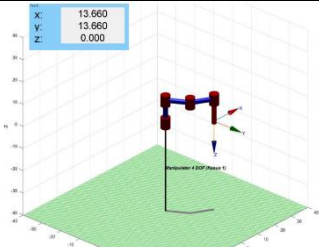
Proceeding of International Joint Conference on UNESA
Homepage : https://proceeding.unesa.ac.id/index.php/pijcu
e-ISSN : 3032-3762

PIJCU, Vol. 2, No. 2, June 2025
Page 1-8
© 2025 PIJCU:
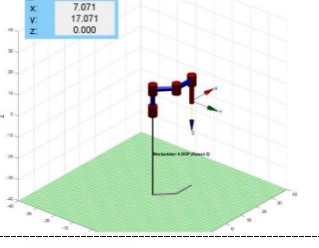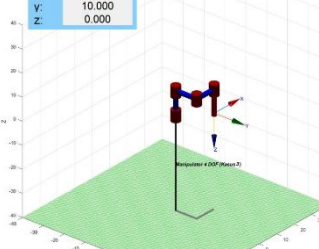Proceeding of International Joint Conference on UNESA
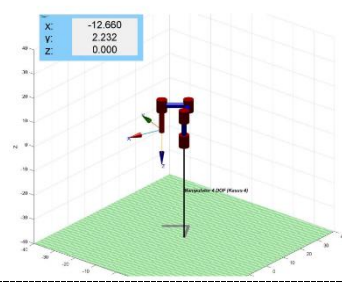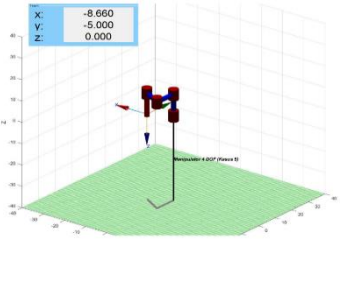
3.4   Case

As in Figure 3, each robot's arm or join have to provide the degree of freedom to move regarding the given rotation angle. Based on this, the following is an example of a robotic arm case determined by varying the rotation angle of each joint.

Table 3. The various variations in rotation angles are solved using manual analysis.

No	θ_2	θ_3	θ_4	End Effector Position (cm)
1	30°	30°	30°	[13,66 13,66 0]
2	45°	45°	0°	[7,07 17,07 0]
3	0°	90°	0°	[10 10 0]
4	120°	100°	30°	[−12,66 2,23 0]
5	−90°	−120°	30°	[−8,66 −5 0]

Table 4. The Visualization and Analysis results with various variations in rotation angles (as Tabel 3) by MATLAB

No	Visualisation Result	Discussion	
		Angle Variation	End Effector Result
1		$\theta_2 = 30°$ $\theta_3 = 30°$ $\theta_4 = 30°$	$\begin{bmatrix} 13,660 \\ 13,660 \\ 0 \end{bmatrix}$
2		$\theta_2 = 45°$ $\theta_3 = 45°$ $\theta_4 = 0°$	$\begin{bmatrix} 7,071 \\ 17,071 \\ 0 \end{bmatrix}$
3		$\theta_2 = 0°$ $\theta_3 = 90°$ $\theta_4 = 0°$	$\begin{bmatrix} 10 \\ 10 \\ 0 \end{bmatrix}$

Proceeding of International Joint Conference on UNESA
Homepage : https://proceeding.unesa.ac.id/index.php/pijcu
e-ISSN : 3032-3762

PIJCU, Vol. 2, No. 2, June 2025
Page 1-8
© 2025 PIJCU:
Proceeding of International Joint Conference on UNESA

4		$\theta_2 = 120°$ $\theta_3 = 100°$ $\theta_4 = 30°$	$\begin{bmatrix} -12{,}66 \\ 2{,}232 \\ 0 \end{bmatrix}$
5		$\theta_2 = -90°$ $\theta_3 = -120°$ $\theta_4 = 30°$	$\begin{bmatrix} -8{,}660 \\ -5 \\ 0 \end{bmatrix}$

Based on Tabel 3 and Tabel 4, it shows that the overall rotational motion influences the end effector of the transforming robot motion. For the cases, when the sum of angle for each link ($\theta_2 + \theta_3 + \theta_4$) is same but different for each θ_2, θ_3, and θ_4, we found that the end effector of the robot is different for each case.

CONCLUSION

Based on the results of the analysis and discussion, we can conclude that regarding the equation of the forward kinematics equation for the motion of the robot arm (manipulator) with 4-DoF obtained are as equation (10). The visualization of the system can be shown in Figur 3 and Tabel 4. Thus, the overall rotational motion influences the position of the end effector of the robot. For the cases with the same number of angles but with different θ_2, θ_3, and θ_4, it turns out that the end effector of the robot is different for each case.

REFERENCES

Faiq, M., Satriatama, W., and Halim, L. (2022). Perancangan awal dan simulasi lengan robot 3 derajat kebebasan berbasis Arduino yang dikontrol dengan aplikasi. *Jurnal Mechanical Engineering Mechatronics*, *7*(2), 118–130.

Gallardo-Alvarado, J., Rodriguez-Castro, R., Perez-Gonzalez, L., and Aguilar-Najera, C. R. (2018). Kinematics of the 3(RPSP)-S fully spherical parallel manipulator by means of screw theory. *Robotics, 7*(2). https://doi.org/10.3390/robotics7020029

Ge, D. (2022). Kinematics modeling of redundant manipulator based on screw theory and Newton-Raphson method. *Journal of Physics: Conference Series, 2246*(1), 012068. https://doi.org/10.1088/1742-6596/2246/1/012068

Hari Purwoto, B., Rindhani Rhokhim, D., and Indraswari, D. (2020). Pemodelan robot kinematik manipulator menggunakan Matlab. *Jurnal Teknik Elektro, 20*, 141–146.

Kucuk, S., and Bingul, Z. (2006). Robot kinematics: Forward and inverse kinematics. In *Industrial Robotics: Theory, Modelling and Control* (pp. 5015). Pro Literatur Verlag, Germany / ARS, Austria. https://doi.org/10.5772/5015

Murray, R. M., Li, Z., and Sastry, S. S. (1994). *A mathematical introduction to robotic manipulation* (Vol. 84, No. 788).

Salman, A. E., and Roman, M. (2022). *Robot Kinematics*.

Serrezuela, R. R., et al. (2017). Kinematic modelling of a robotic arm manipulator using Matlab. *International Journal of Engineering Trends and Technology, 12*(7).

Suddin, D., and Nasrullah, B. (2017). Rancang bangun robot manipulator yang bergerak secara translasi dan rotasi. *Jurnal Teknik Mesin, 1*, 151–156.

Utomo, B., and Munadi. (2013). Analisa forward dan inverse kinematics pada robot manipulator. *Teknik Mesin S-1, 1*(3), 1–10.

Yasmini, L. P. B., & Gunadi, I. G. A. (2012). Kajian awal penerapan konsep mekanika pada gerak robot dengan analisis aljabar.

Development of a Smart Laboratory Iot Trainer Kit Based on Raspberry Pi with The Addition of Fire Sensor, Gas Sensor, and RFID and Monitor Screens in The Telecommunications Lab of The Faculty of Engineering Unesa

Hikmat Oka Kusuma[1*], Gitud Sudarto[1]
[1*] Universitas Negeri Surabaya, Surabaya, Indonesia

ABSTRACT (9 pt)

Keywords:
RFID technology
IoT concepts
Raspberry Pi
Fire Sensor

Integrating IoT concepts into education is critical, and the creation of intelligent IoT lab trainers plays a vital role in this process. This paper outlines the creation of a sophisticated laboratory IoT Trainer kit utilizing a Raspberry Pi. The Telecommunications Lab of Surabaya State University's Faculty of Engineering has fire and gas sensors, RFID technology, and monitoring screens. This trainer facilitates remote monitoring and control of network-connected equipment. The Raspberry Pi microcontroller offers automatic tracking and fast response to potential hazards such as fire or gas leaks by combining computer vision-based sensors and gas/fire detectors. This technique uses a research and development (R&D) structure which includes planning, development, evaluation, and improvement stages. Hardware design, sensor integration, power management, and testing processes are crucial. This prototype is an interactive educational tool fostering comprehension of IoT concepts among students and consumers. Integrating with the Telegram Bot API makes it possible to actively monitor and receive real-time notifications, thereby enhancing laboratory security and efficiency. The successful development of this Trainer improves the standard of IoT teaching and practical training in the academic setting.

INTRODUCTION

One of the goals of the Internet of Things (IoT) concept is to enhance the benefits of continuously connected internet connectivity (Melor, 2018). Buildings can use computer networks to remotely control electronic equipment using the Internet of Things (IoT) (Wegner, 2016). We must be able to use, learn, and apply these technological advances daily. The development of technology that can be used is an example. Electronic equipment such as room lights can be accessed through mobile phones with an internet connection (Bassily et al., 2007). Thus, remote control technology will allow users to monitor and control the lights anytime and anywhere by keeping records in locations with adequate internet networks. Internet of Things (IoT) systems make controlling other electronic equipment easy remotely (Kumar et al., 2019). Due to its many benefits, automation systems have become more prevalent in recent times (Gréczi & Berecz, 2019). One of them is a remote controller over the network. The Raspberry Pi is a microcontroller with a Wi-Fi network chip that allows users to communicate with the system over the same or different networks, depending on the user's needs (Joshi et al., 2015). The user can communicate with the system through the web or phone applications, depending on the situation. Researchers use the idea of the Internet of Things (IoT) to make equipment in telecommunications Laboratories into automated systems (Rusimamto, et al., 2021).

They proposed a Raspberry Pi microcontroller to integrate computer vision-based sensors with gas and flame sensors for sensing and surveillance.

For example, it is used as a room detector; fire sprinkler lights and water will self-ignite without human assistance if a fire or gas leaks occur. One of the technologies that can be used to drive ICT is the innovative laboratory, where all physical devices and laboratory components will be integrated and embedded into electronic devices, making them behave like the Internet of Things (IoT) (Gavali et al., 2016). Used to help monitor and manage laboratory and classroom spaces in real-time (Boelens et al., 2017). Intelligent Laboratory Products begins by gathering information to learn more about the product to develop. Monitored conditions and electrical equipment in laboratories controlled by Smart laboratories are examples of intelligent laboratory products. After the information is collected, an analysis of the need to produce the product is carried out (Coskun & Işik, 2009). After that, system planning is required. Design software and hardware are components of this system (Spector et al., 2015). Hardware design includes applying sensors and actuators to the Raspberry Pi microcontroller using the basic rules of the microcontroller (Sugoyono, 2016). Further analysis of data pins is needed to determine whether they are analog or digital, and the process involves the entire design ecosystem. Using an intelligent digital laboratory will allow many things to be monitored and controlled (Arifianto, et al., 2018). These include air conditioning control, light control, door locks, lab door supervision, and room air temperature and humidity. In addition, the working principle of Passive infrared (PIR) sensors can be used to determine whether a laboratory is being used or not (Habibi & Agustini, 2022).

This Smart Laboratory system has many sensors and actuators that can be used depending on the availability of facilities in the Faculty of Engineering Surabaya State University Telecommunications Lab. They physically connect to the Raspberry Pi, but the sensors generate data that observers can trigger to perform certain actions in specific situations. The system has sensors and actuators that measure and operate in real-time. Using Computer Vision technology, the camera module is used as a human presence sensor. The PIR Sensor also detects people, temperature, and humidity with the DHT sensor, and the phone app is used to monitor the data in real-time.

To solve the problem, the system will be connected to the internet via an Android phone. The research entitled The development of Raspberry Pi-based IoT Smart Laboratory Trainer Kit with the addition of fire, gas, and RFID sensors and monitor screens in the Faculty of Engineering Surabaya State University Telecommunications Lab was appointed based on the background presented.

RESEARCH METHOD

This study employs the research and development (R&D) methodology. Research and development (R&D) is a strategic method that prioritizes creating, experimenting, and enhancing novel products, technologies, or innovations to fulfill requirements and attain targeted objectives (Nurseto, 2012).

Planning stage: During this phase, the researcher establishes the study's objectives, identifies the requirements, and defines the scope of the study. It is crucial to arrange the development steps per the study's objectives carefully.

Development stage: The researcher generates a novel product or technology following a predetermined plan during this phase. A prototype or preliminary model is constructed for testing and evaluation during this project phase.

Evaluation stage: Following the creation of the original prototype or model, the new product or technology undergoes testing to identify possible enhancements and modifications. During the improvement stage, the researcher addresses any issues or shortcomings in a new product or technology by making necessary tweaks and enhancements to enhance its quality and performance. This procedure can be iterated until the product or technology achieves the required level of excellence.

Improvement stage: If a new product or technology has deficiencies or problems, the researcher makes improvements and adjustments to improve its quality and performance. This improvement process can be repeated until the product or technology reaches the desired level of perfection.

Implementation stage: occurs following the successful evaluation and improvement of the product or technology. This stage is conducted to implement the study's findings in the appropriate setting or context. The objective of this implementation phase is to conduct a comprehensive evaluation of the product or technology and assess its reception by the environment or users.

Research Flow Chart

The research process that will be carried out is as follows in the flow chart in Figure 1. This stage of the Literature study involves collecting and analyzing literature related to the research topic to understand pre-existing theories and knowledge. The literature study also helps direct research in the right direction and find gaps in knowledge. Literature test, this stage tests and ensuresthat the literature used as a research reference is correct. The researcher verifies the veracity and relevance of the literature used in the study. Software and Hardware design, this stage involves creating a design for the software and hardware components that will be used to construct the system or tool under study. This design encompasses the technical, architectural, and design specifications of the system or tool that will be constructed.

Raspberry Pi, is a developed mini-computer that serves as the control center of the developed system. Different types of sensors used in research are shown here, such as flame sensors, gas sensors, and RFID sensors. Various actuators, such as servos, relays, and motors, drive or control the system. A breadboard is a place to assemble and connect electronic components temporarily. The GPIO Expansion section showcases the development of GPIO (General Purpose Input Output), which allows the Raspberry Pi to communicate with more devices and components. This design provides a visual overview of the layout and integration of components in the acrylic board media used in the study. The purpose of this design is to provide guidance and reference for developing

the physical system. After the acrylic media is printed, the next step is to install the components according to the layout arranged on the acrylic board media Design. Where the components are all correctly and orderly assembled according to the planned design. To ensure that the components are connected and set correctly, the components are installed carefully. After the components are installed, the next step is the wiring process. This process connects electronic components to acrylic board media using cables or jumper wires. This process aims for each component to communicate and interact according to a pre-planned system design. This process must be carried out carefully and thoroughly because mistakes can lead to damage.
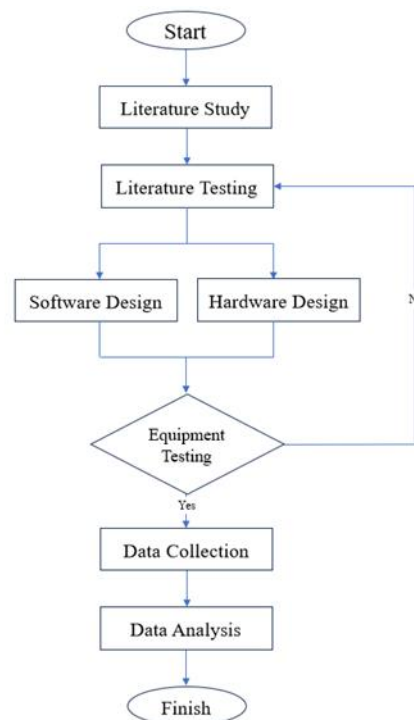

Figure 1. Research Flow Chart.

For the Raspberry Pi model 3B+, the recommended power source is 5V 2.5 A. However, in certain situations, such as when multiple loads require more power, the author uses a power source with 5V 3A. We do this to ensure that the Raspberry Pi has enough power to handle the additional load the other connected components require. In addition, the Raspberry Pi has a cooling fan and heatsink to improve performance and prevent its temperature from being too high when used with high loads. This Trainer uses two types of power — AC power as the main plug and DC power for the Raspberry Pi. AC power is equipped with a switch so that users can adjust the power that goes to the Trainer, and DC power is equipped with a switch that can adjust the power that goes directly to the Raspberry Pi.

All power sensors (VCC and GND) are connected directly to the power during wiring to avoid excessive use of jumper cables during learning. With a direct connection, the wiring

process becomes faster and more orderly, and the problem of unstable connection is minimized. All steps taken to regulate the power supply on this instructor are aimed at ensuring that the Raspberry Pi and other components get enough stable power supply to work correctly and efficiently in any learning or testing. After connecting and setting up the power supply is completed, the next step is to test the tool to ensure that the entire system and components on the instructor are working correctly.

At the equipment testing stage, the system or tool ensures its performance meets expectations and specifications. If there is a problem or discrepancy, the problem will be addressed at the design stage. The tool can be tested in several stages. This includes functionality testing. At this stage, each component is tested individually to ensure the tool works correctly. After components are tested individually, integration testing is performed to ensure that all components can interact with each other and work together in a single system. For example, test how the Raspberry Pi interacts with sensors and actuators and how data from the sensors can be displayed on the LCD monitor screen. After all the tests are completed, the test results should be recorded and analyzed to evaluate the performance of the Internet of Things Smart Laboratory instructor. If a problem or repair is needed, repairs or adjustments are made to ensure the system operates correctly and meets the study's objectives. The data collection stage involves collecting data from testing tools or systems that have been built. The results of tests and observations about the performance of the appliance or system are included in this data collection. Data analysis encompasses qualitative and quantitative methods, helps interpret research results, and draws conclusions.

RESULTS AND DISCUSSION

Raspberry Pi, is a developed mini-computer that serves as the control center of the developed system. Different types of sensors used in research are shown here, such as flame sensors, gas sensors, and RFID sensors. Various actuators, such as servos, relays, and motors, drive or control the system. A breadboard is a place to assemble and connect electronic components temporarily. The GPIO Expansion section showcases the development of GPIO (General Purpose Input Output), which allows the Raspberry Pi to communicate with more devices and components. This design provides a visual overview of the layout and integration of components in the acrylic board media used in the study. The purpose of this design is to provide guidance and reference for developing the physical system. After the acrylic media is printed, the next step is to install the components according to the layout arranged on the acrylic board media Design. Where the components are all correctly and orderly assembled according to the planned design. To ensure that the components are connected and set correctly, the components are installed carefully. After the components are installed, the next step is the wiring process. This process connects electronic components to acrylic board media using cables or jumper wires. This process aims for each component to communicate and interact according to a pre-planned system design. This process must be carried out carefully and thoroughly because mistakes can lead to damage.
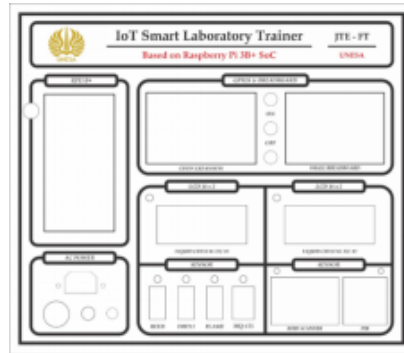
Figure 2. Acrylic Board Design

For the Raspberry Pi model 3B+, the recommended power source is 5V 2.5 A. However, in certain situations, such as when multiple loads require more power, the author uses a power source with 5V 3A. We do this to ensure that the Raspberry Pi has enough power to handle the additional load the other connected components require. In addition, the Raspberry Pi has a cooling fan and heatsink to improve performance and prevent its temperature from being too high when used with high loads. This Trainer uses two types of power—AC power as the main plug and DC power for the Raspberry Pi. AC power is equipped with a switch so that users can adjust the power that goes to the Trainer, and DC power is equipped with a switch that can adjust the power that goes directly to the Raspberry Pi.

Figure 3. Prototype Trainer

All power sensors (VCC and GND) are connected directly to the power during wiring to avoid excessive use of jumper cables during learning. With a direct connection, the wiring process becomes faster and more orderly, and the problem of unstable connection is minimized. All steps taken to regulate the power supply on this instructor are aimed at ensuring that the Raspberry Pi and other components get enough stable power supply to

work correctly and efficiently in any learning or testing. After connecting and setting up the power supply is completed, the next step is to test the tool to ensure that the entire system and components on the instructor are working correctly.

At the equipment testing stage, the system or tool ensures its performance meets expectations and specifications. If there is a problem or discrepancy, the problem will be addressed at the design stage. The tool can be tested in several stages. This includes functionality testing. At this stage, each component is tested individually to ensure the tool works correctly. After components are tested individually, integration testing is performed to ensure that all components can interact with each other and work together in a single system. For example, test how the Raspberry Pi interacts with sensors and actuators and how data from the sensors can be displayed on the LCD monitor screen. After all the tests are completed, the test results should be recorded and analyzed to evaluate the performance of the Internet of Things Smart Laboratory instructor. If a problem or repair is needed, repairs or adjustments are made to ensure the system operates correctly and meets the study's objectives. The data collection stage involves collecting data from testing tools or systems that have been built. The results of tests and observations about the performance of the appliance or system are included in this data collection. Data analysis encompasses qualitative and quantitative methods, helps interpret research results, and draws conclusions.

This Trainer method has been used and tested to ensure it works well. These instructors can help students understand basic and advanced concepts about the Internet of Things (IoT) through various application examples and experiments. In addition, the instructor is wrapped in a special suitcase designed to be easy to carry and use. The suitcase is designed to store the instructor safely and neatly. The Smart Laboratory IoT Trainer is small and portable, allowing users to perform IoT learning and experiments in various locations. At the Telecommunications Systems Laboratory of the Surabaya State University, the findings of this study help improve education and understanding of Internet of Things (IoT) technologies. This Trainer can be an effective and interactive learning tool to help students and other users understand and grasp more IoT concepts.

Integration with Telegram Bot API
Figure 4 shows the result of integrating the tool with the Telegram Bot API. Telegram bots provide relevant information from sensors that have been installed, even when they are not on the internet. The Sensor also alerts a group of Telkom lab members if a hazard, such as a gas leak or fire, is detected. In conclusion, by integrating the Telegram Bot with sensor data, Telkom lab members can be monitored and alerted in real-time to quickly respond to dangerous situations remotely. This improves the safety and efficiency of using equipment in the telecommunication laboratory.
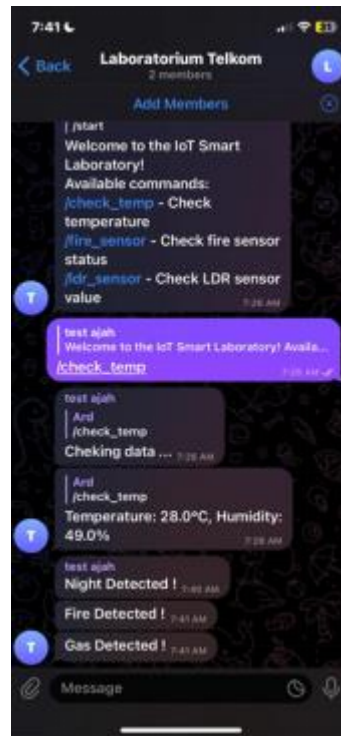
Figure 4. Integration Result of IoT

CONCLUSION

Studies show that developing Raspberry Pi-based Smart IoT laboratory instructors in the Telecommunications Systems Laboratory of the Surabaya State University was successful. The previous Smart Laboratory IoT Trainer, created in 2023, was well-developed and used. Users can learn Internet of Things (IoT) concepts and applications effectively and interactively with these instructors. The test showed that the Trainer system works well and gives the best results. Using a 5V 3A power supply along with a heatsink and cooling fan on the Raspberry Pi helps system stability and prevents overheating when the system works with high loads. Because it is packed in a special suitcase, this Trainer is also easier to use and carry anywhere. This makes it easy for users to explore and learn about IoT in various places.

REFERENCES

Arifianto, H., Adi, K., & Widodo, C. E. (2018). Design of automatic bottle filling using Raspberry Pi. *Jurnal Fisika: Uji Coba dan Aplikasi*, 1(1), 10. https://doi.org/10.14710/jpa.v1i1.3910

Bassily, H., Sekhon, R., Butts, D. E., & Wagner, J. (2007). A mechatronics educational laboratory – Programmable logic controllers and material handling experiments. *Mechatronics*, 17(9), 480–488. https://doi.org/10.1016/j.mechatronics.2007.06.004

Boelens, R., De Wever, B., & Voet, M. (2017). Four key challenges to the design of blended learning: A systematic literature review. *Educational Research Review*, 22, 1–18. https://doi.org/10.1016/j.edurev.2017.06.001

Coskun, I., & Işik, M. F. (2009). Design and application of the technical training set for PLC-based power supply unit developed for industrial applications. *Procedia - Social and Behavioral Sciences*, 1(1), 1658–1662. https://doi.org/10.1016/j.sbspro.2009.01.293

Gavali, A. B., Patil, S. A., & Koli, A. R. (2017). Technology-based learning system in programmable logic controller education. In *Proceedings of the IEEE 8th International Conference on Technology for Education (T4E 2016)* (pp. 264–265). https://doi.org/10.1109/T4E.2016.071

Gréczi, P., & Berecz, A. (2019). Opportunities of Raspberry Pi's use in education. *Journal of Applied Multimedia*, 13(3), 73–79. https://doi.org/10.26648/jam.2018.3.001

Joshi, A., Kale, S., Chandel, S., & Pal, D. (2015). Likert scale: Explored and explained. *British Journal of Applied Science & Technology*, 7(4), 396–403. https://doi.org/10.9734/bjast/2015/14975

Kumar, S., Tiwari, P., & Zymbler, M. (2019). Internet of Things is a revolutionary approach for future technology enhancement: A review. *Journal of Big Data*, 6(1). https://doi.org/10.1186/s40537-019-0268-2

Melor Md Yunus. (2018). Digital platforms, online corpora, mobile learning and BYOD (bring your own device), online CPD (continuous professional development) and the global staffroom. *2(1)*, 33–34.

Nurseto, T. (2012). Membuat media pembelajaran yang menarik. *Jurnal Ekonomi dan Pendidikan*, 8(1), 19–35. https://doi.org/10.21831/jep.v8i1.706

Rusimamto, P. W., Wijayanto, E., & Fadhilah, D. M. (2021). Fluid mixing process based on programmable logic controller as training kit for electrical engineering education students. *International Journal of Integrated Engineering*, 13(4), 104–111. https://doi.org/10.30880/ijie.2021.13.04.009

Spector, J. M., Merrill, M. D., Elen, J., & Bishop, M. J. (2014). *Handbook of research on educational communications and technology: Fourth edition* (4th ed.). Springer. https://doi.org/10.1007/978-1-4614-3185-5

Sugyono. (2016). *Metode penelitian kuantitatif, kualitatif, dan R&D* (1st ed.). Alfabeta.

Wagner, J. (2016). Meet the Raspberry Pi. In *Raspberry Pi® User Guide* (pp. 11–22).

Yunus, M. M. (2018). Digital platforms, online corpora, mobile learning, and BYOD (bring your own device), online CPD (continuous professional development), and the global staffroom. *Journal of Digital Learning and Education*, 2(1), 33–34.

Dryer Cabinet Modification with Heating Element

M T Santoso[1*], G Sudarto[2], H Saputra[3]
[1, 2, 3*] Universitas Negeri Surabaya, Surabaya, Indonesia

ABSTRACT (9 pt)

Keywords:
Dryer cabinet
Gas emission
Electric heating
Food Technology

The modification of a gas-powered drying machine into an electric-powered drying machine in the Food Technology laboratory of the Family Welfare Education Department Faculty of Engineering Surabaya state of University aims to make the use of tools more effective, efficient and improve the work function of the tools. Gas dryers are more energy intensive and less practical to use. Apart from that, the distribution of hot air from gas dryers is less even. Electric powered dryers use electric heating elements as heat producers and are more environmentally friendly because they do not produce gas emissions. The electric heating element used is a tubular type heating element equipped with a ceramic insulator as safety. Hot air is distributed in the drying machine by a blower placed close to the heating source. Even distribution of hot air and a stable temperature are the keys to speed in drying. This research is research and development research. The expected result of this research is that the tool can function optimally, effectively and efficiently. Drying carried out on bay leaves with a capacity of 500 gr using an electric heating temperature of 60-70 C can dry the material in less than 5 hours.

INTRODUCTION

Drying is a method of preserving food ingredients by reducing the liquid content through evaporation with the help of heat (Asiah and Djaeni., 2021). There are various methods of drying. The natural method of drying is using direct sunlight. The food to be dried is cut or placed in such a way on a tray or base and placed in an open area under direct sunlight. During the drying process, the outside air around the material will rise due to radiant heat from the sun which then comes into contact with the wet material (Osman, 2018). Initially the temperature of the material will increase and cause the water to evaporate until the material becomes drier (Apriandi et al., 2022). This phenomenon is the basis for the development of drying technology, where parameters (flow rate, temperature and humidity) are controlled to obtain dry material with the desired moisture content. Another method of drying, namely the artificial drying method, is drying with the help of drying equipment (Purnamasari et al., 2019). There are several drying equipment, namely solar dryers, cabinet dryers, tunnel dryers and so on. This drying equipment can help the drying process using gas or electricity and even sunlight energy. Each tool certainly has advantages and disadvantages, so development of the tool's working methods is needed to minimize deficiencies so that the drying process is more effective and efficient (Arhamsyah et al., 2018). The food technology laboratory in the Culinary Study Program, Family Welfare Education Department, Faculty of Engineering, Surabaya State of University has several cabinet type drying equipment. The dryer cabinet uses gas fuel. Gas-powered cabinet dryers have several disadvantages, including uneven drying temperatures, less environmental friendliness, high equipment maintenance costs and complicated work methods. Thus, it is necessary to improve the performance of the tool so that its use is more effective and efficient. Modification is generally defined as an attempt to change or adapt. However, specifically modification

is an effort made to create and display something new, unique and interesting (Saputra, 2015). The modifications referred to in this research are changes to unit components that support tool performance with the aim of optimizing tool performance so that it can produce higher quality products effectively and efficiently. Modification of the dryer cabinet by changing the unit type from a gas-powered dryer cabinet to a dryer cabinet using an electric heating element. The aim of this research is to modify a cabinet type dryer to improve the performance of the tool so as to create a more effective and efficient artificial dryer that saves energy, short drying time, is safe and has a simpler working method.

RESEARCH METHOD

The research method used is the research and development (R&D) method. Research and development methods are research methods used to produce certain products, and test the effectiveness of these products (Okpatrioka, 2023). Development research is a process or steps to develop a new product or improve an existing product (Hakim et al., 2017). The following are the research procedures.

Potential and Problems

This research begins with a potential or problem. High frequency of tool use and suboptimal tool maintenance result in decreased tool performance. The gas flow in the dryer cabinet is not smooth due to a clogged burner nozzle so that the lighter does not work and the tool cannot be used. Apart from that, there are problems with the unstable temperature control system. This obstacle can certainly hamper laboratory activities. Procurement of equipment every year has also not been realized so a development of tool working methods is needed to improve tool performance.

Data Collection

Literature studies can be used as material for planning certain products that are expected to overcome problems. Through literature studies, the scope of a product will be studied, the breadth of use, supporting conditions so that the product can be used or implemented optimally, as well as its advantages and limitations. Literature studies are also needed to find out the most appropriate steps in developing the product.

Product Design

The final result of this activity is a new product design complete with specifications. This design is still hypothetical because its effectiveness has not been proven, and will be known after going through tests. The product design must be realized in pictures or charts, so that it can be used as a guide for assessing and making it, and will make it easier for other parties to understand it.

    2.3.1   Hardware design is the initial activity in dryer cabinet modification product design. Hardware design includes preparing tools and materials, designing designs, measuring and assembling electric heating elements, assembling boxes for placing wiring and electronic modules, assembling fans, timers and temperature sensors.

2.3.2   Software design includes the process of setting the temperature sensor system, setting the timer system, setting the electric heating element and setting the blower.

Design Validation
Validate the design of the product by experts or food technology lecturers, electrical lecturers and culinary lecturers to determine the effectiveness of the dryer cabinet product.

Design Revision
This activity is based on input from experts regarding the shortcomings of the product design. Researchers are tasked with improving product designs based on directions from experts.

Product Testing
Product testing in this research is by testing the function of tool components including testing the timer function compared to a stopwatch to determine the precision or accuracy of time measurements. Apart from that, tests were carried out on the temperature sensor function compared to a mercury temperature thermometer as well as product function tests for drying.

Product Implementation
After passing the trial use phase, the dryer cabinet can be implemented in student practicum activities. Researchers continue to evaluate the performance of the tool during use. The following is a research design flow chart in Figure 1.
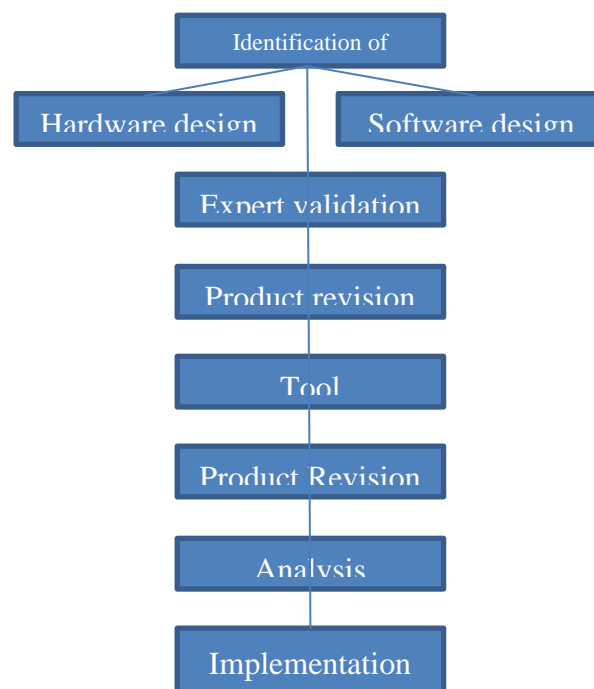
Figure 1. Research steps with bibliometric analysis

The research design is intended to provide direction for researchers regarding procedures for carrying out R and D research. The following is a picture of the design of a dryer cabinet with heating elements.
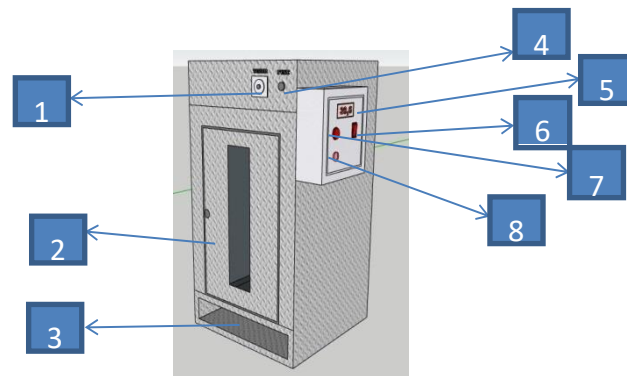

Figure 2. Dryer Cabinet with Heating Element

Information :
1. Timer
2. Heating Elemen
3. Fan
4. Fuse
5. Temperature control
6. Power
7. Indicator lamp

RESULTS AND DISCUSSION

The result of this research is a prototype dryer cabinet with heating elements. Based on research by Jesika, Amnur and Luqman, ovens should use low power heaters to save more electricity (Osman, 2018). The heating element used is the finned heater type, namely a heating element with finned pipes. The Finned heater is straight in shape with a tube length of 50 cm with a diameter of 11 mm and a voltage of 220 volts 250 watts. The fins on the heating element pipe function to collect the heat produced and then radiate the heat to the air medium. According to research by Meriadi, Selamat and Muhammad, [9]to meet the requirements for work safety due to electricity, the heating element must last a long time at the desired temperature, have strong construction, a small expansion coefficient and a small temperature coefficient so that the working current is constant. When installing the heating element, it is equipped with a ceramic insulator to protect it from electrical currents. This is in accordance with Meriadi's research (2018) that heat protection materials are mainly ceramic insulating materials. Finned heaters are installed vertically on the right and left sides of the dryer cabinet (Meriadi et al., 2018). The dryer cabinet is equipped with a blower to remove hot air inside the cabinet in an effort to speed up the reduction in air temperature and also evenly distribute the hot air throughout the

area inside the cabinet. This is in accordance with Jesika, Amnur and Luqman's research (2018) that the heating element (heater) produces hot air which will be distributed into the air with the help of a fan or blower. The heat will spread evenly with the help of the blower. There is a timer to set the drying time and also a temperature sensor to regulate the temperature required for drying. In the tool performance test, the timer system ran normally. The times shown are compared with the appropriate stopwatch. Likewise with temperature sensor trials compared with mercury thermometers. In testing the performance of the tool for drying bay leaves, the time needed to dry 500 gr of bay leaves was 5 hours at a temperature of 60'C. Drying is even on all shelves because the heating elements are located vertically on the right and left sides of the cabinet and are assisted by a fan or blower in evenly distributing the hot air. Meanwhile, based on Andika and Eka's research (2022) drying machines with gas stove heaters produce different heat temperatures on each shelf or uneven heat and quite high drying costs (Bakara and Daryanto, 2022). Based on Antu's research (2021), conventional drying using solar heat is faster and more effective than drying using a dryer (Khasanah et al., 2021).

CONCLUSION

Modified dryer cabinets with heating elements are more effective than dryer cabinets with stove heating. In terms of energy use, a cabinet dryer with heating elements consumes 250 watts of electrical energy for 5-8 hours of use. Cabinet dryer with stove heating consumes 3 kg of gas resources in 2 days of use for 5-8 hours. So energy consumption by a dryer cabinet with a heating element is more efficient compared to a dryer cabinet with a gas stove heater. Another advantage is that dryer cabinets with heating elements do not produce fuel emissions like stove heaters, so they are more environmentally friendly. The working procedure for a cabinet dryer with a heating element is simpler and safer. There is a button to turn on the unit then the blower will automatically rotate to adjust the temperature settings which can be adjusted according to needs and a timer system to set the drying time if needed. Maintenance of dryer cabinets with heating elements is cheaper and easier.

REFERENCES

Apriandi, N., Aprilliansyah, R., Ramadhan, Y., Harahap, M., Saputra, F. A., & Bakar, S. (2022). Karakterisasi alat pengering tipe kabinet berbahan bakar liquefied petroleum gas (LPG) dengan penambahan low-cost material heat storage (LCMHS). *Jurnal Rekayasa Mesin*, 17(2), 281.

Arhamsyah, M., Syam, H., & Jamaluddin, J. (2018). Modifikasi mesin pengering dengan memanfaatkan udara panas dari elemen pemanas listrik. *Jurnal Pendidikan Teknologi Pertanian*, 4, 196.

Asiah, N., & Djaeni, M. (2021). *Konsep dasar proses pengeringan pangan*.

Bakara, A. A., & Daryanto, E. (2022). Rancang bangun mesin pengering kopi tipe rak dan penyangrai kopi tipe roaster dengan pemanas kompor gas. *Jurnal Engineering Development*, 2(1), 1–7.

Hakim, E. Z. R., Hasan, H., & Syukriyadin, S. (2017). Perancangan mesin pengering hasil pertanian secara konveksi dengan elemen pemanas infrared berbasis mikrokontroler Arduino Uno dengan sensor DS18B20. *Jurnal Karya Ilmiah Teknik Elektro*, 2(3), 16–20.

Khasanah, R., Nurdianingsih, E., Pradana, A. B., & Siswanto, A. (2021). Studi literatur: Pengering jagung dengan elemen pemanas menggunakan sensor DHT11 dan sensor kadar air berbasis Arduino Uno. *Jurnal Teknik Elektro*, 10(1), 163–171.

Meriadi, M., Meliala, S., & Muhammad, M. (2018). Menggunakan pemanas listrik. *Jurnal Energi Elektrik*, 7, 47–53.

Okpatrioka, O. (2023). Research and development (R&D): Penelitian yang inovatif dalam pendidikan. *Jurnal Pendidikan, Bahasa dan Budaya*, 1(1), 86–100.

Osman, J. E. (2018). Rancang bangun oven pintar. *Proceeding 6th Applied Business Engineering Conference*, October, 197–206.

Purnamasari, I., Meidinariasty, A., & Hadi, R. N. (2019). Prototype alat pengering tray dryer ditinjau dari pengaruh temperatur dan waktu terhadap proses pengeringan mie kering. *Jurnal Kinetika*, 10(3), 25–28.

Saputra, I. (2015). Modifikasi media pembelajaran pendidikan jasmani sekolah dasar. *Jurnal Pendidikan*, 17(2), 28–35.

Friction Welding Machine Design

Suhadi [1*], Ronny Tuhumena [1]
[1*] Department of Engineering, Universitas Negeri Surabaya, Surabaya, Indonesia

ABSTRACT

Keywords:
Friction Welding
Hydraulics
Friction
Rotation
Pressure

The development of welding science is increasingly rapid in the fields of construction, vehicle component manufacturing, electrical component manufacturing. Welding that is currently developing is friction welding and also friction stir welding. The use of Friction Welding is to combine two shafts using a Friction Welding machine as an example of a vehicle axle component (Shaft), repairing a broken axle, and currently there have been many studies from lecturers and students about Friction Welding with publications in national and international journals. The design of the Friction Welding machine is made by modifying the tail stock on a lathe which functions as a pressing tool. The design process first studies the work of the lathe then designs the actuator (hydraulic pressing tool) using a hydraulic system to obtain axial pressure using a piston as a forge when the friction welding process is carried out. From the design results, the diameter of the hydraulic cylinder is 85 mm, the diameter of the piston rod is 30 mm and the piston stroke is 200 mm using the piston diagram, force and pressure which means that the hydraulic cylinder is safe to use.

INTRODUCTION

Background

The development of welding science is related to technology that is also increasingly developing. Both in the fields of construction, vehicle component manufacturing, electrical manufacturing. Welding that is currently developing is friction welding and also friction stir welding. The use of Friction Welding is to combine two shafts using a Friction Welding machine as an example on vehicle axle components (Shaft), repairing broken axles, and currently there has been a lot of research from lecturers and students about Friction Welding with publications in national and international journals.

The results of the researcher's observations are that the Friction Welding Machine currently used for research by lecturers and students is a lathe that has been modified with the addition of a hydraulic system (as a press/forge when connecting two shafts).

Based on the identification of the problems above, the researcher took the initiative to conduct research, namely Designing a Friction Welding Machine Without Modifying a Lathe Machine.

Objectives

1. Design and build a Friction Welding machine that is useful for research by lecturers and students in the Department of Mechanical Engineering, Surabaya State University.
2. Can be used as a practical for mechanical engineering students to learn about various welding methods.

RESEARCH METHOD

Type of Research

The approach method used in this research is experimental analysis research which aims to design and make a friction welding machine using a lathe.

The use of this method is based on the research problem to be used, the research objectives and the research process according to the desired research results and objects.

Location

The research locations are:

a. Manufacture of Friction Welding Machine, namely a pressing tool and hydraulic system in the machining laboratory of the mechanical engineering department of Surabaya State University.

b. Assembly of Friction Welding Machine in the Machining Laboratory of the Department of Mechanical Engineering, Surabaya State University.

c. Friction Welding Machine Testing in the machining laboratory of the mechanical engineering department of Surabaya State University.

Research Design

Research design is the steps and stages carried out by researchers in an effort to create tools and analyze the tools created.
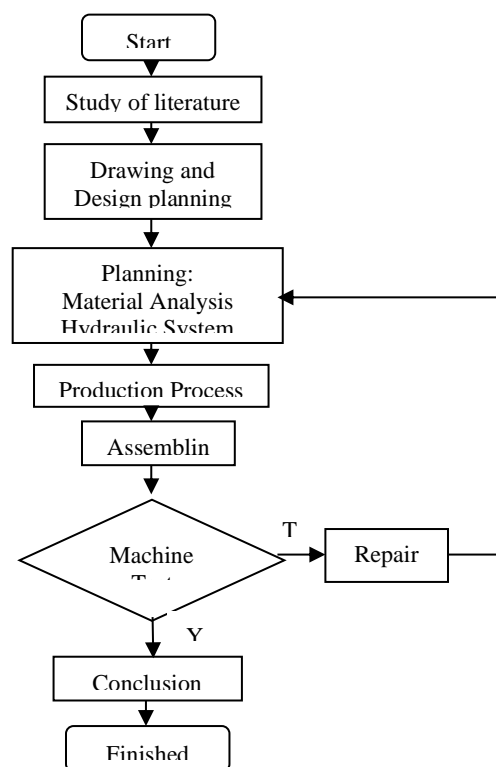
```
┌───────────┐
│   Start   │
└─────┬─────┘
      ▼
┌──────────────────┐
│ Study of literature│
└─────┬────────────┘
      ▼
┌──────────────────┐
│   Drawing and    │
│  Design planning │
└─────┬────────────┘
      ▼
┌──────────────────┐
│    Planning:     │◄────────────┐
│ Material Analysis│             │
│ Hydraulic System │             │
└─────┬────────────┘             │
      ▼                          │
┌──────────────────┐             │
│ Production Process│             │
└─────┬────────────┘             │
      ▼                          │
┌──────────────────┐             │
│    Assemblin     │             │
└─────┬────────────┘             │
      ▼         T    ┌─────────┐ │
    ╱ Machine ╲─────►│ Repair  │─┘
    ╲  Test   ╱      └─────────┘
      │ Y
      ▼
┌──────────────────┐
│   Conclusion     │
└─────┬────────────┘
      ▼
┌──────────────────┐
│   Finished       │
└──────────────────┘
```

Figure 1. Flowchart Research

RESULTS AND DISCUSSION
Result
Hydraulic Press Tool Design
Therefore, a press tool with a hydraulic mechanism was designed to replace the tail stock. This tool is placed in the position where the Tail Stock is placed on the lathe. As in the Figure 2.

Figure 2. Tail Stock

Based on the shape and size of the Tail Stock, a replacement design for the Tail Stock can be designed using a hydraulic system as shown in Figure 3.
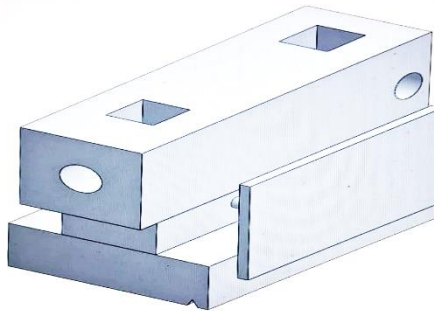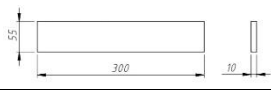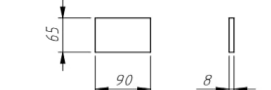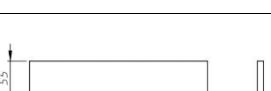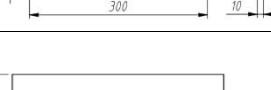

Figure 3. 3D Drawing

Drawing and Work Process
In the process of making a hydraulic press tool (actuator) there are several things that need to be considered, namely: preparing materials, preparing the tools/machines to be used, understanding the work diagram and following the sequence of work steps.

NO	Draw	Work
1		Saw Machine Lathe Welding machine
2		Saw Machine Lathe
3		Saw Machine Milling machine Welding machine
4		Saw Machine Milling machine Welding machine

5		Saw Machine Milling machine Welding machine
6		Saw Machine Milling machine Welding machine
7		Saw Machine Milling machine Welding machine
8		Saw Machine Milling machine Welding machine
9		Saw Machine Milling machine Welding machine
10		Saw Machine Milling machine Welding machine
11		Saw Machine Milling machine Welding machine
12		Saw Machine Milling machine Welding machine

The production process carried out is the sawing process (raw materials), the turning process, the grinding process and finally the welding process. Once completed, the next step is to assemble the hydraulic press machine, namely installing the piston and lathe chuck.

Figure 4. Hydraulic Press Machine

Hydraulic System
The circuit used in the hydraulic system functions as a press.

NO	Component Name	Size	Information
1	Hydraulic cylinder	Dp: 85mm, Dst: 30, Stroke: 200 mm	*Double Acting Cylinder*
2	steering valve	*Hand Path* Type	4/3

Friction Welding Machine Design

3	Hydraulic pump	10 MPa (1000 Mpa)	*Gear Pump*
4	Flexible Hose	3/8 inch	SAE 100 R2 DI
5	Hydraulic tank	40 liters	
6	Electric motor	3 *phase AC*	1HP, 1400RPM
7	Appropriate	*MPT Double Nipple*	3/8 inch

The designed hydraulic system looks like Figure 5.

Figure 5. Hydraulic System

This study uses the CHIA-GA lathe on the Unesa lathe because it has a mechanical brake system that becomes an electric brake where when braking the spindle stops and cuts off the electric current to the electric motor to prevent overloading as shown in Figure 6.

Component	Specification
Brand	CHIA, GA
Spindle speed	1800 Rpm
Tailstock travel	100mm
Tail taper	MT 3
Electric motor	1 HP

Figure 6. The System

a. Stages of friction welding process:
  1) Adjustment of hydraulic press tool with lathe chuck. In this adjustment, two pieces of tapered iron are used which are clamped in the hydraulic press chuck and clamped in the lathe chuck which is set in the middle, namely parallel to the two sharp angles with the distance between the specimens to be tested for welding.
  2) Tighten the bolts and nuts so that the hydraulic press machine does not move or shift as in Figure 7.

Figure 7. Setting Center

3) Friction welding process.
4) The lathe rotation setting is 1800 Rpm.
5) Adjust the hydraulic pump pressure on the hydraulic press by adjusting the valve lever and pressure gauge.
6) Mount both specimens in the chuck of the press tool and the chuck of the lathe.
7) The welding process is by turning on the lathe with the desired rotation of 1800 Rpm and the position of the chuck on the press tool does not rotate, attach it to the surface of both ends of the shaft then move the valve lever slowly forward to create friction pressure which will result in heating the surface of both specimens by providing pressure called tempering pressure so that a connection occurs between the two specimens. After the connection occurs, wait a few seconds then the lathe is run. brake and turn off the lathe and remove the welding specimen as shown in Figure 8.

Figure 8. Friction Welding Process

The stages of testing specimen material are as shown in the table.

Table 1. Specimen Material

NO	Material	Example	Diameter	Long	Rpm	Time
1	St 41	1	20	100	1800	30
2	St 41	2	20	100	1800	30
3	St 41	3	20	100	1800	30
4	St 41	4	20	100	1800	30

Discussion
Based on friction welding testing, the results obtained are:

NO	Example	Picture
1	1	

2	2	
3	3	
4	4	

From the friction welding results using the hydraulic press tool design (actuator), it can be concluded that there must be improvements in the binding of the hydraulic press tool holder to the lathe bed because the design for the bed holder is made the same as the Tail Stock holder and the influence of hydraulic pressure (Forging) prevents burning of both shafts in the friction welding results.

CONCLUSION

The overall result of the friction welding machine design process can be concluded that the design of this friction welding machine is designed as follows:

1. Hydraulic press tool (actuator).

There is a design improvement because the fastener connecting the actuator to the lathe bed is not tight, the design is adjusted to the tail stock of the lathe machine

2. Hydraulic System

NO	Component Name	Size	Information
1	Hydraulic cylinder	Dp: 85mm, Dst: 30, Stroke: 200 mm	*Double Acting Cylinder*
2	steering valve	*Hand Path* Type	4/3
3	Hydraulic pump	10 MPa (1000 Mpa)	*Gear Pump*
4	Flexible Hose	3/8 inch	SAE 100 R2 DI
5	Hydraulic tank	40 liters	
6	Electric motor	3 *phase AC*	1HP, 1400RPM
7	Appropriate	*MPT Double Nipple*	3/8 inch

REFERENCES

Firmansyah, M. R. G., & Puspitasari, R. P. (2018). Analysis of rotational speed, friction duration and pressure on tensile strength of friction welding results. *Journal of Tech. Machines and Learning*, 1(2), 1–5.

Haryanto, P., Cahyono, B., & Supandi. (2018). Testing tensile strength on friction welding joints of steel joined using friction welding machine research results: Friction

welding (friction welding, FW) the joining process occurs due to the heat generated by heating between two metal surfaces. In *Seminar Proceedings*.

Husodo, N., Sanyoto, B. L., Bangun, S., & Mahirul, S. (2013). Application of friction welding technology in the framework of joining two pieces of carbon steel St41 in back spring pin products. *Journal of Energy and Manufacturing*, *6*(1), 43–52.

Mortensen, F., Jensen, K. S., & Loose, L. C. (2001). Mechanical and microstructural properties of inertia-friction welded 416 stainless steel. In *Proceedings* (pp. 268–273).

Pujono, D., Prabowo, D., & Pratama, E. P. (2019). Friction machine prototype design and construction. *Bangun Rekaprima*, *5*(05), 13–20.

Satyadianto, D. (2015). *The effect of variations in friction pressure, forging pressure and friction duration on impact strength in friction welding joints using AISI 4140 alloy steel*.

Upara, M. A. N. (2019). Strength analysis of rotary friction welding joints of bronze material with stainless steel based on ASME standard. In *Seminar and Conference Proceedings*.

Soft Starting of Induction Motors in Traditional Oil Mining Using Arduino Uno

Harrij Mukti K[1], Rohmanita Duanaputri[2*], Rachmat Sutjipto[3], Muhammad Fahmi Hakim[4], Ahmad Hermawan[5], Abdillah Toha Yusuf[6], Rifqi Nanda Prayoga[7]

[1,2*,3,4,5,6,7] Politeknik Negeri Malang, Surabaya, Indonesia

ABSTRACT (9 pt)

Keywords:
Soft starting,
Induction motor,
Arduino Uno,
Oil mining,
Energy efficiency,
Sustainability

High energy consumption during the starting process of induction motors is a significant challenge in traditional oil mining operations. Starting current surges not only cause mechanical stress and instability of the power grid, but also result in substantial energy waste. The use of a soft starting method with Arduino Uno offers a potential solution to address these issues. A soft starting system was designed and tested using Arduino Uno as the control platform, aiming to provide a controlled and environmentally friendly approach to motor start-up. Tests were conducted under various loads to assess energy savings and sustainability improvements. Results showed that the method successfully reduced the initial current surge to approximately 150% of the rated current, compared to 500% in direct starting (DOL). The implementation of this system is a significant step towards a more environmentally friendly and energy-efficient oil extraction method, contributing to improved motor reliability, reduced energy consumption, and increased efficiency and sustainability in traditional oil mining practices.

INTRODUCTION

Induction motors are crucial in traditional oil mining due to their cost-effectiveness, easy maintenance, and high reliability (Sen, 2021). However, they face a significant challenge during startup: a current surge up to seven times the nominal value, which can stress components, affect reliability, and increase energy consumption (Rashid, 2014).

To address this, efficient power regulation systems like soft starting have emerged. Soft starting allows gradual motor start, reducing initial current surges (Chapman, 2012). This method not only protects the motor and maintains electrical network stability but also contributes to energy efficiency and sustainability in industrial operations. Studies show soft starting can reduce start-up energy consumption by up to 30% compared to conventional methods (de Almeida et al., 2014).

The Arduino Uno microcontroller, known for its versatility and ease of use, has gained popularity in automation and control systems (Margolis et al., 2020). Its low cost and robustness make it suitable for harsh conditions in oil mining. Integrating Arduino Uno in soft starting systems for induction motors offers precise control, allowing parameter adjustments based on specific motor characteristics and load conditions, thus optimizing energy use and promoting sustainable operations (Wildi, 2006). Soft starting significantly reduces mechanical wear and tear, leading to longer operational life and decreased downtime (Rodriguez et al., 2007). This increased durability and efficiency contribute to the overall sustainability of oil mining operations by reducing equipment replacement needs and minimizing energy waste.

Recent research by Mukti et al. (2024) modeled oil extraction with a 48 kW motor power as 15 W with a 2 kg load. Their subsequent study developed an induction motor usage system for traditional oil mining, successfully designing a braking system for the

Wonocolo oil mines. This followed their earlier work replacing combustion engines with electric motors. However, field reports indicate ongoing issues, including motors failing to start or having difficulty starting, and frequent MCB tripping during startup.

These challenges underscore the importance of implementing effective soft starting systems in traditional oil mining operations. By addressing the high starting currents and associated issues, such systems can significantly improve motor reliability, reduce energy consumption, and enhance the overall sustainability of oil extraction processes. The integration of affordable and robust control devices like Arduino Uno presents a promising approach to achieving these goals, particularly in remote and harsh environments typical of traditional oil fields.

RESEARCH METHOD

The research to be conducted aims to develop a soft starting device for 3-phase induction motors. The entire research process and its implementation are described in the following flowchart:
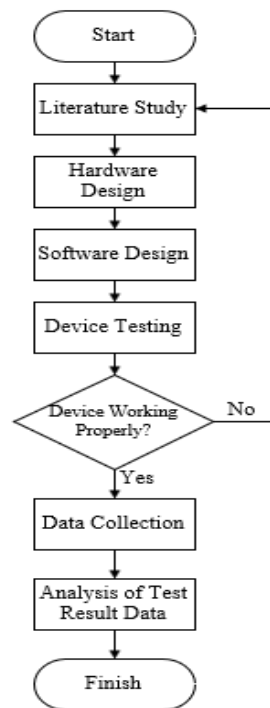

Figure 1. Research process flowchart

Circuit Design

This device uses 3-phase 380 V and 5 V DC for the Arduino microcontroller, obtained by transforming one phase from 220 VAC to 5 VDC. The system includes an MCB for protection and a contactor controlled by a push button. A TRIAC, regulated by Arduino, manages the soft starting process. The Arduino receives commands via Bluetooth from an Android app through an HC-05 module. It uses a Zero Crossing Detector for AC sine wave detection and displays the ignition time on an LCD screen. The TRIAC gradually increases motor voltage, with changes monitored by an Ampere + Voltmeter. A TOR protects the motor from overload. The overall circuit can be seen in **Figure 2** below.
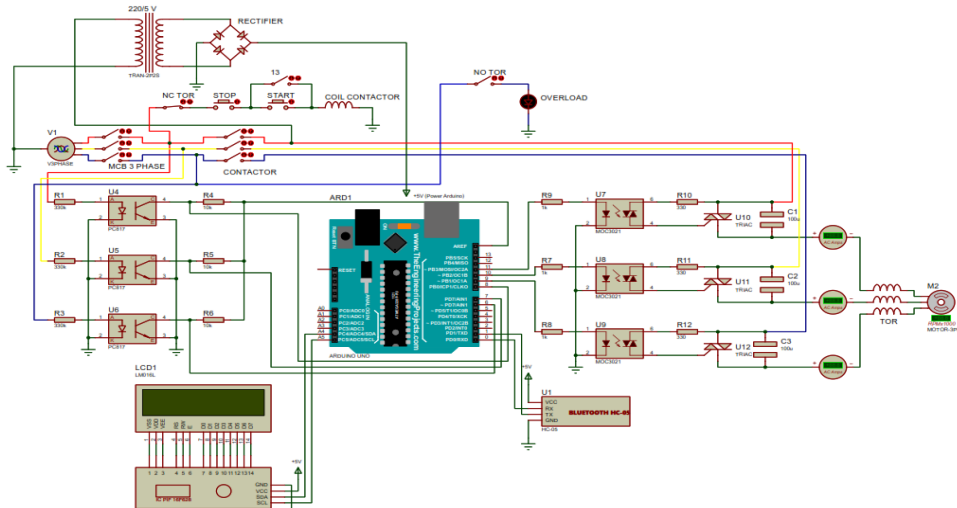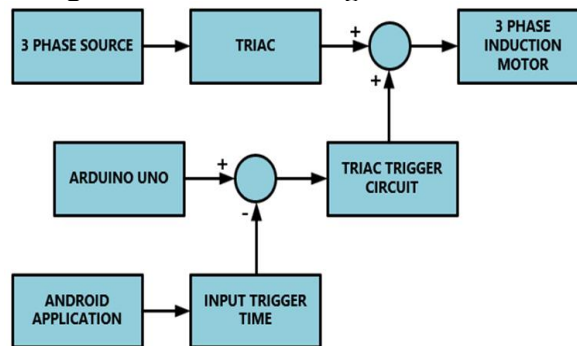
Figure 2. Overall design of the circuit

Figure 3. Block diagram of the circuit

Based on the **Figure 3**, 3-phase power source is used as a voltage source to drive the motor. The voltage entering the motor will be controlled by the TRIAC, where in order to distribute the TRIAC voltage, a trigger mechanism is required that is controlled by Arduino. In regulating the TRIAC triggering, Arduino also requires a control mechanism that is obtained through Bluetooth signal input from the Android Application. The signal input sent from the application to the Arduino is the trigger time that will be given to the TRIAC so that the TRIAC can work to regulate the ignition time.

Data Collection

The motor that will be used in this research is a squirrel cage rotor motor type with a power capacity of 0.33 HP or 0.25 kW. When an experiment was carried out using a motor, it was found that it took 10 seconds to lift the load to the top, so it can be seen that the amount of power released by the motor to the load was 3.92 W. Then, when torque measurements were carried out, the result show that the motor connected to this load had a torque of 0.0249 Nm. Data was taken within a period of 15 seconds, with details of 10 seconds during the starting process and the next 5 seconds after the soft starting process is complete to determine if instability occurs during steady-state conditions. The load used for testing is a model of a traditional petroleum mining system. The load has a mass of 2 kg and a height of 2 m.

RESULTS AND DISCUSSION

This section discusses the results of soft starting tests on traditional oil mining modeling.

Measurement Result

After the measurement process is complete, data is obtained as in **Table 1**. The blue column is the time area where the soft starting process has been completed and the motor is rotating at its nominal voltage and speed.

Table 1. Soft starting measurement results

Time	Voltage (V)						Current (A)			RPM	P
(s)	R-S	S-T	T-R	R-N	S-N	T-N	R	S	T		(W)
1	0	0	0	0	0	0	0	0	0	0	0
2	70	73	132	0	11	12	0,65	0,79	0,69	1,6	33,1
3	230	240	108	85	115	111	0,81	1,14	1,03	69,2	97,3
4	231	206	260	127	127	112	1,08	1,11	1,14	668,9	132
5	161	183	227	110	105	101	1,14	1,17	1,17	796,9	113
6	172	181	149	103	98	95	1,16	1,18	1,17	1007,8	100,1
7	252	175	244	102	109	108	1,15	1,15	1,17	1298,7	132,3
8	211	212	226	153	155	156	1,19	1,16	1,15	1352,1	129
9	232	188	257	134	124	125	1,16	1,12	1,12	1439,5	130
10	391	405	393	199	233	228	0,94	0,88	0,89	1467,1	182
11	407	400	403	225	238	225	0,85	0,94	0,96	1493,9	188,9
12	399	402	399	225	221	229	0,87	0,94	0,96	1493,2	188,8
13	405	400	402	221	222	221	0,86	0,94	0,96	1493,8	189,2
14	401	408	399	228	222	222	0,86	0,94	0,96	1493,1	189,4
15	402	401	400	230	222	222	0,86	0,94	0,96	1493,4	188,6

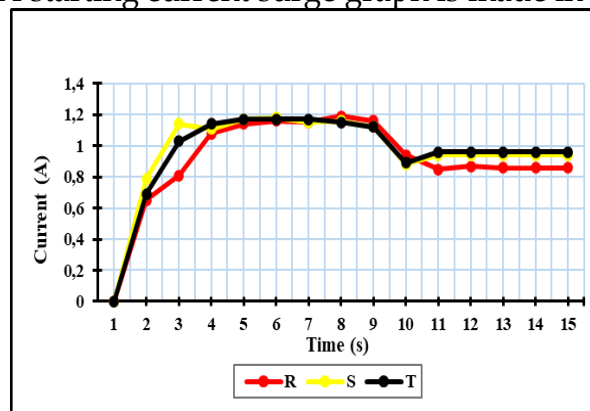Based on the **Table 1**, A starting current surge graph is made in **Figure 4** below.

Figure 4. Current increase graph

Analysis of Starting Current Characteristic

The graphic in **Figure 4** shows a gradual increase in current. The current peaks at about 150% of nominal in 4-9 seconds, then stabilizes with a slight increase due to motor load. There is a slight imbalance between phases (R, S, T), which is common in three-phase systems.

The maximum current reaches 1.2-1.3 A, much lower than the direct starting method, reducing stress on components and minimizing voltage drops. The small fluctuations in current at steady state are likely due to load characteristics or control system interaction. Similar patterns across all phases indicate good system balance and consistent soft starter performance. The current is stable after starting, indicating successful control system operation. The soft starting system handles load characteristics well, without significant current spikes.

Comparative Analysis with DOL Starting

To validate the effectiveness of this soft starting method, a comparative analysis is needed with other starting methods, namely the Direct On-Line (DOL) method. The DOL method was chosen as a comparison because it has the largest current surge characteristics among other starting methods, so that the difference in current characteristics will be easier to observe. In DOL starting, current surges generally occur in a very short duration, especially if the motor has a relatively small power. In this motor, the duration of the current surge only occurs in 0.3 seconds as seen in **Figure 5.**
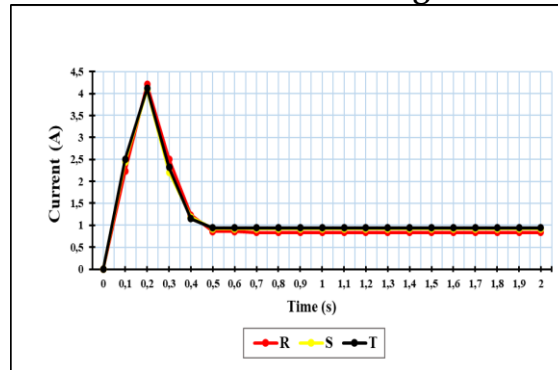

Figure 5. Current characteristics in DOL starting

Analysis of Figure 4 and Figure 5 shows the characteristic differences between the DOL and soft starting methods. In the DOL method, a current surge occurs up to 500% of the nominal current (about 4-4.2 A), but only lasts for a short time for 300-400 milliseconds. In contrast, soft starting produces a lower current surge, about 150% of the nominal current, but lasts longer, about 6 seconds (from the 3rd to the 9th second).

Impact on Reducing Energy Consumption

The implementation of soft starting for induction motors in traditional oil mining operations demonstrates significant potential for reducing energy consumption. By controlling the starting current and voltage applied to the motor, soft starting minimizes energy waste during the motor's acceleration phase.

Our comparative analysis with DOL starting showed that the soft starting method limits the current surge to approximately 150% of the nominal current, compared to 500% in DOL starting. This significant reduction in peak current directly translates to lower energy consumption during start-up. The gradual voltage increase applied by the soft starter results in a more efficient use of energy during acceleration, contrasting with DOL starting where full voltage is applied immediately, leading to energy waste in the form of heat and mechanical stress.

Increased Sustainability due to Reduced Energy Consumption

The implementation of soft starting for induction motors in traditional oil mining has a dual positive impact on industrial and environmental sustainability. From the industrial perspective, the technology improves operational efficiency and extends equipment life by reducing mechanical stress. This reduces the frequency of equipment replacement, which in turn minimizes environmental impacts related to manufacturing and disposal. From an environmental perspective, reduced energy consumption directly reduces greenhouse gas emissions and reduces stress on local ecosystems. The technology also contributes to improved air quality, water conservation, and reduced habitat disturbance around mining sites.

The precision control capabilities of Arduino-based soft starters allow for detailed motor performance data collection and analysis, which can be used for further optimization.

The adoption of this energy-efficient technology is also in line with global sustainability goals and increasingly stringent environmental regulations.

Overall, the use of soft starting creates a ripple effect of sustainability benefits that extend from the industrial sector to the wider environment, helping the oil and gas industry improve its sustainability practices.

CONCLUSION

The developed module successfully performed the soft starting and DOL starting processes on a 3-phase induction motor quite well, although there was current imbalance and voltage fluctuation occur during its process. In the soft starting method, the current surge reached 150% of the nominal current for 6 seconds, while the DOL method produced a higher surge (500% of the nominal) but only lasted 0.3 seconds. This difference in characteristics shows the advantage of soft starting in reducing stress on the motor's electrical and mechanical systems, which has the potential to extend equipment life and reduce maintenance costs. Furthermore, the implementation of soft starting on induction motors in traditional oil mining not only significantly reduces energy consumption, but also improves the sustainability of the industry and the environment through emission reduction, resource conservation, and ecosystem protection. These dual benefits create an effective solution to improve operational efficiency while minimizing environmental impacts, thus making a positive contribution to more sustainable mining practices in the long term.

ACKNOWLEDGEMENTS (OPTIONAL)

REFERENCES

Sen, P. C. (2021). *Principles of Electric Machines and Power Electronics, International Adaptation*. John Wiley & Sons.

Rashid, M. H. (2021). Power Electronics: Devices, Circuits and Applications. *TIDEE: TERI Information Digest on Energy and Environment*, 20(2), 277-277.

J Chapman, S. (2004). Electric Machinery Fundamentals. *5th ed*. New York, NY: McGraw-Hill Education.

De Almeida, A. T., Ferreira, F. J., & Both, D. (2014). Technical and economical considerations in the application of variable-speed drives with electric motor systems. *IEEE Transactions on industry applications*, 41(1), 188-199.

Margolis, M., Jepson, B., & Weldin, N. R. (2020). *Arduino cookbook: recipes to begin, expand, and enhance your projects*. O'Reilly Media.

Wildi, T. (2006). *Electrical Machines, Drives, and Power Systems*. Pearson Educación.

Rodriguez, J., Pontt, J., Silva, C. A., Correa, P., Lezana, P., Cortés, P., & Ammann, U. (2007). Predictive Current Control of a Voltage Source Inverter. *IEEE transactions on industrial electronics*, 54(1), 495-503.

Mukti, H., Duanaputri, R., Ridzki, I., & Hakim, M. F. (2024). Braking System for a 3-phase Induction Motor in Traditional Petroleum Mining. *International Journal of Electrical Engineering and Applied Sciences (IJEEAS)*, 7(1).